Supplementary Information

Material and methods

Cultivation of strains. All *E. coli* DH10B strains (Supplementary Table 6), *E. coli* BL21 (DE3) without any overexpression plasmids and *Photorhabdus* strains (Supplementary Table 7) used in this study were cultivated in liquid or solid Luria-Bertani (LB, pH 7.0) medium at 30°C. All *E. coli* BL21 (DE3) strains with different overexpression plasmids (Supplementary Table 5) were cultivated in a standard cultivation condition for protein expression (method described below). The cultivation condition for construction of *Photorhabdus luminescens* mutants was described below. Chloramphenicol (34 μg mL^{-1}), ampicillin (100 μg mL^{-1}), kanamycin (50 μg mL^{-1}), streptomycin (50 μg mL^{-1}) and rifampicin (50 μg mL^{-1}) were used for the selection of strains with corresponding resistant markers. For cultivation of *E. coli* strain ES16 in ^{15}N or ^{13}C labeled medium, ISOGRO-^{15}N or ISOGRO-^{13}C medium was prepared according to manufacturer´s instructions (Sigma-Aldrich). Isopropyl-β-D-1-thiogalactopyranoside (IPTG, 0.1 mM) was used to induce the heterologous expression of *ant* genes in *E. coli* BL21 (DE3).

General methods in molecular biology. All methods used in molecular biology were conducted according to standard procedures and manufacturer´s instructions. All oligonucleotides (primers) obtained from Sigma-Aldrich were listed in Supplementary Table 4. All Plasmids constructed in this work were confirmed by sequencing at the SeqIT GmbH (Germany, Kaiserslautern) also listed in Supplementary Table 5. Polymerase chain reactions (PCRs) were performed using the phusion high-fidelity polymerase (Thermo-scientific). DNA isolation was performed with GeneJET™ Gel Extraction Kit (Fermentas). Plasmid isolation was performed with GeneJET™ Plasmid Miniprep Kit (Fermentas). Transformation of plasmids into *E. coli* was carried out using electroporation protocol for *E. coli* in an electroporation cuvette with a width of 1 mm (1250V, 25 μF, 200Ω). Genomic DNA was isolated using Gentra® Puregene® kit (Qiagen) according to the protocol for Gram-negative bacteria. Plasmid ZQ80 was constructed using an artificial gene (synthesized by Life Technologies™) flanked with restriction sited *Eco*RI/*Pst*I.

Construction of *E. coli* strains with different combinations of *ant* genes. Two strategies were used to combine different *ant* genes in this work. The first one is the combination of pJET1.2/blunt and pSU18 based plasmids. The second one is the

combination of pCOLA Duet-1, pACYC Duet-1 and pCDF Duet-1 based plasmids. All *E. coli* strains used in this work (with the respective plasmids) were listed in Supplementary Table 4. Plasmids derived from pJET1.2/blunt and pSU18 vector were transformed into *E. coli* DH10B for heterologous expression of *ant* genes. Plasmids derived from Duet-vectors were transformed into *E. coli* BL21 (DE3) for IPTG induced heterologous expression of *ant* genes.

Heterologous expression of genes in *E. coli* DH10B: for analysis of produced polyketides. First of all, different DNA fragments were amplified using primers in Supplementary Table 4, resulting in *antB*, *antABC*, *antAB*, *antBC* PCR products. The PCR products were then digested with restriction enzymes *Nde*I/*Sac*I and subsequently ligated into pSU18 vector, generating plasmids (Supplementary Table 5) ZQ6, ZQ10, ZQ11 and ZQ16, respectively. The plasmid pSUsfp was cloned using the same method. Later, *antDEFG*, *antDEFGH* and *antDEFGHI* genes were amplified with the primers in Supplementary Table 4. The resulted PCR products were directly ligated into pJET1.2/blunt, generating the plasmids ZQ9, ZQ12 and ZQ13 in Supplementary Table 5. The plasmid pSUmtaA was described previously.[1] All generated plasmids were selectively transformed into *E. coli* DH10B for heterologous expression, yielding strains listed in Supplementary Table 6. The polyketides found in the bacteria culture were listed in Supplementary Table 1.

Cloning, expression, purification, crystallization and structure determination of His_6-AntI His_6-AntI (*Photorhabdus luminescens*, Uniprot: Q7MZT8, expression vector ZQ40 [Supplementary Table 5]) was heterologously expressed in *E. coli* BL21(DE3) gold. Cells were grown in 6 liter LB-cultures in the presence of kanamycin (50 mg/L) at 37°C. Protein production was induced at an OD_{600} of 0.6 by the addition of IPTG to a final concentration of 1 mM. Subsequently, cultures were incubated overnight at 20°C. Cells were harvested by centrifugation and stored at -20°C until further use. SeMet-labeled protein was expressed in the same strain using a protocol previously described[2].

For protein purification, cell pellets were resuspended in buffer A (50 mM tris hydrochloride, 500 mM NaCl, pH 7.5) and 20 mM imidazole. Cell disruption was carried out by sonication (Branson Digital Sonifier 250, G. Heinemann, Schwäbisch Gmünd, Germany). The resulting suspension was centrifuged at 30,000 g for 30 min at 4°C

using a SIGMA 4K15 centrifuge (Sigma Aldrich, Germany). The supernatant was applied to a 5 mL HisTrap™ HP column (GE Healthcare Life Science, Uppsala, Sweden), which had been equilibrated with buffer A (flow rate, 5 mL/min) using an ÄKTA prime plus system (GE Healthcare, Uppsala, Sweden). The column was washed with 50 mL of buffer A containing 50 mM imidazole. Next, the protein was eluted with buffer A containing 200 mM imidazole. Fractions were combined, concentrated and directly applied to a HiLoad™ 16/60 Superdex™ 200 column (GE Healthcare, Uppsala, Sweden), which had been equilibrated with 20 mM Tris pH 7.5, 100 mM NaCl, 1 mM dithiothreitol (DTT). The obtained peak fractions were analysed by SDS PAGE, pooled and concentrated to a final concentration of 10 mg/mL using Amicon Ultra Centrifugal Filter Device (Millipore, Billerica, USA). Protein not directly applied to crystallographic experiments was flash frozen with liquid nitrogen and stored at -80°C.

Native and SeMet labeled His_6-AntI crystals were grown by the sitting drop vapor diffusion method at 20°C combining 0.2 µL protein (10 mg/mL in 20 mM Tris pH 7.5, 100 mM NaCl, 5 mM DTT) and 0.2 µL reservoir (0.1 M NaAc, 0.1 M HEPES pH 7.5, 22% PEG3350). Mountable crystals grew within one week. Native diffraction datasets were collected up to 1.85 Å resolution using synchrotron radiation at the X06SA-beamline, SLS, Villigen, Switzerland (see Supplementary Table 3). Recorded reflections were processed with the program package XDS[3]. His_6-AntI crystallized in the orthorhombic space group $C222_1$ with cell parameters of a = 54 Å, b = 154 Å, c = 91 Å, indicating one AntI-subunit in the asymmetric unit with a solvent content of 41%. Experimental phases were obtained by single anomalous dispersion (SAD) methods using the peak absorption wavelength of selenium derivatized AntI crystal (λ = 0.9798 Å, f' = -8.05; f'' = 5.52). The program package SHELXD[4] located 10 heavy atom sites using a dataset recorded to 1.9 Å resolution. Subsequent SHARP-SAD-phasing[5] and solvent flattening with the program DM[6] resulted in an electron density map with phases at about 2.5 Å resolution. The quality was sufficient to model secondary structure elements by polyalanine residues. The initial model was transferred to the native dataset with a resolution of 1.85 Å by applying rigid body- and preliminary positional-refinement using REFMAC5[7]. The resulting electron density map allowed unambiguous identification of the entire AntI-sequence. The model was completed in iterative rounds with the three-dimensional graphic programs MAIN[8] and COOT[9]. Temperature factors were anisotropically refined with restraints between bonded atoms using translation / libration / screw motion-parameters, yielding crystallographic

values of R_{cryst} = 0.168 and R_{free} = 0.204 (see Supplementary Table 3). Coordinates were confirmed to have superb stereochemistry in the Ramachandran plot with 98.1% of residues in the most favored region and 1.9% of residues in the additionally allowed regions. The asymmetric unit cell contains one AntI subunit with the six N-terminal and the three C-terminal amino acid residues being structurally disordered.

Heterologous expression of genes in *E. coli* BL21 (DE3): for mutagenesis of AntI. ZQ40_S245A, ZQ40_D326A, ZQ40_D327A and ZQ40_H355A harboring the mutated gene *antI**, were generated (Supplementary Table 5). The site-directed mutation was achieved by ligation of two amplified PCR fragments, using the designed primer pair binding around the mutated region (Supplementary Table 4) and a primer pair binding at ColA *ori* (pCOLA Duet-1). The plasmid ZQ40 harboring the original *antI* gene was used as PCR template. The primer pair binding at ColA *ori* is 5`-[Phos]GTGGATTTAGATATCGAGAGTC-3´ and 5´-TAATTCTCAGTTACCAATGGC-3´. For coexpression, plasmid ZQ62 encoding AntDEFGH and plasmid ZQ76 encoding AntABC were constructed using primers in Supplementary Table 4. Transformation of plasmids ZQ40, ZQ62 and ZQ76 into *E. coli* BL21 (DE3) led to strain ES53. Transformation of plasmids encoding mutated AntI* into *E. coli* BL21 (DE3) containing plasmids ZQ62 and ZQ76 led to strains ES59, ES61, ES62 and ES64 in Supplementary Table 6. HPLC-MS analysis is shown in Figure 3b.

Heterologous expression of genes in *E. coli* BL21 (DE3): for coexpression with RED1. RED1 encoded originally by *actVI-ORF1* in *Streptomyces coelicolor* A3(2) was investigated in order to find out whether the polyketide intermediate **1** produced by AntA-H can serve as a substrate for the stereospecific ketoredution.[10] For this experiment, a gene encoding RED1 optimized for expression in *E. coli* was synthesized (Life Technologies™). The artificial gene flanked with restriction sites *Eco*RI/*Pst*I was digested and ligated into pCOLA Duet-1 vector, resulted in plasmid ZQ80 (Supplementary Table 5). Plasmid ZQ62 encoding AntDEFGH and Plasmid ZQ76 encoding AntABC (described above) were used for coexpression with plasmid ZQ80 in *E. coli*, resulting in strain ES65 in Supplementary Table 6.

DNA sequence of the synthesized artificial gene encoding ketoreductase RED1 from the actinorhodin biosynthesis (*actVI-ORF1*):

EcoRI*GAATTC*CATGAGCACCGTTACCGTTATTGGTGCAGGCACCATTGGTCTGGG
TTGGATTAACCTGTTTAGCGCACGTGGTCTGACCGTTCGTGTTAATAGCCGTCG
TCCGGATGTTCGTCGTGTTGTTCATGAAGCACTGGAACTGTTTAGTCCGGGTCG
TGTTGATGAACTGGCAGCACGTATTGAATATGAACCGGATGTGGGTCGTGCAGT
TGCCGGTGCAGATGTTGTTAGCGAAAATGCACCGGATGATCTGCCGCTGAAAC
AGCGTCTGTTTGCAGAAATTGGTGCCGCAGCACCGGATCATGCACTGGTTCTGA
GCAGCACCAGCAAACTGCTGCCGGATGAACTGAGCCGTGATATGCCTGGTCCT
GGTCGTCTGGTTGTTGCACATCCGTTTAATCCGCCTCATATTGTTCCGCTGGTT
GAAGTTGTTCGTGGTGAACGTACCGATCCGGAAGCAGTGGAACGTACCCTGGC
ATTTCTGGCAAGCGTTGGTCGTACACCGGTTGTTGTGCGTCGTGCACTGCCTG
GTTTTGCAGCAAATCGTCTGCAAAGCGCACTGCTGCGTGAAAGCATTCATCTGG
TTCTGGAAGGTGTTGTTACCGTTGAAGAACTGGATCGTATTGTTACCGATAGTAT
TGGCCTGCGTTGGAGCACAATTGGTCCGTTTCATGCATTTCATCTGGGTGGTGG
TCCGGGTGGTCTGCGTAAATGGCTGGAACATCTGGGTAGCGGTCTGGAACAGG
GTTGGCGTGGTCTGGGCCAGCCTGCACTGACACCGCAGGCAGTTGAAGCCCT
GGTTGCACAGACCGAAGCAGCATATGGTCATCGTCCGTATGCAGAACTGGTTC
GTGATCGTGATGATCGTCATCTGGCCGTTCTGGCAGCCCTGGAACGCACCGAA
CAGCCGCAAGAAGAAACCAAATAA*CTGCAG*PstI

Construction of *P. luminescens* mutants. Insertion mutants (*antI*::cat) and the deletion mutant (Δ*antC*) were constructed as described previously.[11]

Analysis of polyketides in bacteria culture by HPLC-MS. For production analysis, extracts from 10 ml of culture were prepared. Usually, 1 % overnight pre-culture was used for inoculation and 2 % AMBERLITE™ XAD-16 (Sigma Aldrich) was added at the same time for the absorption of hydrophobic secondary metabolites. AMBERLITE™ XAD-16 resin beads were collected with a sieve (or filter paper) after 72 h, washed with small amount of water and extracted with 20 mL of methanol. The methanol extract was dried and dissolved in 1 mL methanol, which could be then diluted (1:10-dilution) for the analysis in HPLC-MS. Additionally, the remaining bacteria culture without AMBERLITE™ XAD-16 and bacteria cells was extracted using 10 mL ethyl acetate/acetic acid (99:1). After remove of all the solvent, the dried extract was dissolved in 1 mL methanol, which could be then diluted (1:10-dilution) for the analysis in HPLC-MS.

Analysis of extracts was performed on Dionex ULTIMATE 3000 HPLC system with a photodiode array detector in the range of 200-600 nm and an Acquity UPLC BEH C18 column (1.7 µm, Waters), which is coupled to Bruker AmaZon X iontrap mass spectrometer using electrospray ionization at positive and negative mode. Solvent A: water with 0.1 % formic acid and solvent B: acetonitrile with 0.1 % formic acid. Gradient A: 5 % solvent B for 2 min, increasing to 95 % solvent B in 12 min, 95 % solvent B for 3 min. Gradient B: 10 % solvent B for 4 min, increasing to 25 % in 9 min, increasing to 95 % solvent B in 1 min, 95 % solvent B for 3 min. Flow rate: 0.6 mL min^{-1}. Gradient A was used as standard gradient for most analysis in this work. Gradient B was used for separation of **SEK4**, **SEK4b**, **mutactin** and **SEK34** (Supplementary Table 2).

Biochemical assays. Hydrolase AntI activity assays were performed with synthesized model compounds **S1**-**S4** (Supplementary Figure 6). The methyl esters (**S2** and **S4**) were hydrolyzed *in situ* with 250 µM NaOH solution with a final concentration of 2 mM for synthetic analogs. The assays with the four model compounds (2.5 µM, **S1**-**S4**) were realized with 250 µM His_6-AntI in Tris-HCl (pH 8). The same assays were performed without His_6-AntI as negative controls. After incubation for 3 h at 30°C, the reaction was stopped by the addition of 200 µL ACN to the mixture. After centrifugation, the clear supernatants were analysed by HPLC/MS analysis quantifying the formation of **S5** (m/z 221 $[M+H]^+$). Results showed that model compounds **S1** and **S3** (Figure 3c) could not be converted by His_6-AntI. For the conversion of **S2** to **S5**, no significant difference with or without AntI could be observed even for shorter incubation times of 1 h.

Synthesis of S2. 145 mg of methyl 2-(3,5-dimethoxyphenyl)acetate (**i**) were dissolved in 5 ml of acetic acid, then 540 µl of acetic anhydride and 3 drops of $HClO_4$ were added to the mixture. A yellow precipitate appeared. The mixture was heated to 35°C for 7 min. The completion of the reaction was monitored by TLC. The acid was quenched with ice and 20 ml of saturated $NaHCO_3$. The aqueous layer was extracted 3 times with 10 ml of Et_2O. The organic layers were combined and extracted with 20 ml of brine and then dried over Na_2SO_4. The solvents were removed under vacuum. The crude product was purified by flash chromatography with a gradient from 40-80 % EtOAc in hexane over 10 column volumes. After evaporation of the solvents, 120 mg of **S2** were

obtained as yellow oil. ^{1}H NMR (500 MHz, $CDCl_3$) δ 6.31 (dd, *J* = 30.1, 2.1 Hz, 2H), 3.76 (s, 3H), 3.74 (s, 3H), 3.62 (s, 2H), 3.61 (s, 3H), 2.46 (s, 3H). ^{13}C NMR (126 MHz, $CDCl_3$) δ 203.77, 171.77, 161.61, 159.45, 134.97, 123.64, 108.27, 97.50, 55.62, 55.42, 51.97, 39.10, 32.24. HRMS (ESI) Calcd for $C_{13}H_{17}O_5$: 253.1070 $[M+H]^+$, Found: 253.1089 $[M+H]^+$.

Synthesis of ii. 565 mg of methyl ester **i** (2.7 mmol, 1 equiv.) were dissolved in 8.5 ml of dry toluene under nitrogen. The mixture was then cooled down to -78°C and 2.8 ml of Me_3Al in hexane (2M, 2.8 mmol, 1.03 eq.) was added. 1.55 g of tert-butyl((1-methoxyvinyl)oxy)dimethylsilane (7.57 mmol, 2.83 equiv.) were dissolved in 2 ml of toluene. This solution was slowly added to the reaction mixture. The mixture was warmed to 0°C and stirred for 7 hours. The mixture was quenched with 100 ml of saturated aqueous solution of $NaHCO_3$, and then extracted 3 times with 30 ml of EtOAc. The organic layers were combined und washed once with brine, then dried over Na_2SO_4. The solvent removed under vacuum and the residue oil was purified by flash chromatography using a gradient from 5-40 % of EtOAc in hexane over 10 column volumes. The two diasteroisomers of **ii** were isolated, 250 mg of diastereoisomer A (22% of yield) and 120 mg of diastereoisomer B (11%) were obtained both as yellow oil. Isomer A: ^{1}H NMR (250 MHz, $CDCl_3$) δ 6.44 (d, *J* = 2.3 Hz, 2H), 6.21 (t, *J* = 2.3 Hz, 1H), 3.64 (s, 6H), 3.54 (s, 3H), 3.20 (s, 3H), 3.02 (dd, *J* = 33.6, 13.1 Hz, 2H), 2.44 (dd, *J* = 45.5, 14.2 Hz, 2H), 0.78 (s, 9H), 0.02 (d, *J* = 9.1 Hz, 6H). Isomer B: ^{1}H NMR (250 MHz, $CDCl_3$) δ 6.44 (d, *J* = 2.3 Hz, 2H), 6.21 (t, *J* = 2.2 Hz, 1H), 3.64 (s, 6H), 3.54 (s, 3H), 3.20 (s, 3H), 3.02 (dd, *J* = 33.6, 13.1 Hz, 2H), 2.44 (dd, *J* = 45.4, 14.2 Hz, 2H), 0.78 (s, 10H), 0.02 (d, *J* = 9.1 Hz, 6H). ^{13}C NMR (63 MHz, $CDCl_3$) δ 170.33, 160.30, 139.51, 108.96, 100.80, 98.73, 55.28, 51.44, 49.05, 44.50, 41.52, 25.86, 18.34, -2.67, -2.90.

Synthesis of iii. 160 mg of **ii** was dissolved in 16 ml of MeOH, and 8 ml of HCl 6M were added at 0°C. The mixture was stirred 30 min at 0°C then the ice bath was removed and the mixture was stirred for 1 hour at room temperature. The mixture was quenched with 100 ml of $NaHCO_3$ and extracted three times with 25 ml of AcOEt. The organic layers were combined, washed with brine and dried over Na_2SO4. The solvents were removed under vacuum and the crude was purified by flash chromatography. The expected compound **iii** (63 mg) was obtained as yellow oil with

a yield of 60%. ^{1}H NMR (500 MHz, $CDCl_3$) δ 6.37 (d, *J* = 2.2 Hz, 1H), 6.34 (d, *J* = 2.2 Hz, 2H), 3.77 (s, 6H), 3.73 (s, 2H), 3.71 (s, 3H), 3.46 (s, 2H). ^{13}C NMR (126 MHz, $CDCl_3$) δ 197.78, 165.06, 158.59, 132.71, 105.02, 104.81, 96.86, 52.80, 52.77, 49.84, 47.84, 45.18.

Synthesis of S4. 30 mg of **iii** were dissolved in 0.190 ml of acetic acid, then 180 µl of acetic anhydride and two drops of $HClO_4$ were added to the mixture. The mixture color turned to orange. It was heated to 35°C for 5 min. The completion of the reaction was monitored by TLC. The acid was quenched with ice and 20 ml of saturated NaHCO3. The aqueous layer was extracted 3 times with 10 ml of Et_2O. The organic layers were combined and washed with 10 ml of brine and then dried over Na_2SO_4. The solvents were removed under vacuum. The crude product was purified by flash chromatography with a gradient from 40-80 % EtOAc in hexane over 10 column volumes. After evaporation of the solvents, 12 mg of **S4** (yield: 36%) were obtained as a slight purple solid. ^{1}H NMR (500 MHz, $CDCl_3$) δ 6.35 (d, *J* = 2.2 Hz, 1H), 6.23 (d, *J* = 2.2 Hz, 1H), 3.78 (s, 3H), 3.77 (s, 2H), 3.75 (s, 3H), 3.67 (s, 3H), 3.51 (s, 2H), 2.41 (s, 3H). ^{13}C NMR (126 MHz, $CDCl_3$) δ 203.00, 199.83, 167.92, 162.03, 160.14, 135.60, 122.76, 108.83, 97.69, 55.62, 55.46, 52.31, 48.59, 48.27, 32.29. HRMS (ESI) Calcd for $C_{15}H_{19}O_6$: 295.1176 $[M+H]^+$, Found: 295.1184 $[M+H]^+$.

Multiple sequence alignments of hydrolases. All performed multiple sequence alignments were calculated using the ClustalW-algorithm[12] applying the standard parameters.

Molecular dynamics (MD) simulations. Classical molecular dynamics (MD) simulations were performed with compound **1** modelled in different poses into the crystal structure of the *apo*-form of AntI. The ligand-protein system was solvated and neutralized in a water-ion box with a 150 mM KCl concentration, comprising in total *ca*. 59,000 atoms. The CHARMM36 force field[13] was employed to model the protein, the water molecules, and the ions. Different reaction intermediates (substrate, Bürgi-Dunitz intermediate, product, see main text) of the ligand were parametrized using a combination of the CGenFF force field[14] and *in-house* DFT-based parameters computed at B3LYP/def2-SVP level. The MD simulations were performed at *T* = 310 K and *p* =1 bar in an *NPT* ensemble, using an integration timestep of 2 fs. Long-range

electrostatic interactions were treated by the Particle Mesh Ewald (PME) method. All residues were modeled in their standard protonation states, except for His355 and Asp287, which were modeled in their protonated forms. The different ligand poses were relaxed for 100 ns. The MD simulations were performed with NAMD2[15], and VMD[16] was used for analysis and visualization.

DFT calculations. DFT models were built based on classically relaxed structures of the substrate:AntI complex. The DFT models comprised the aromatic rings of the substrate and the S-acyl moiety of its PPT-arm, the sidechains of protein residues Ser245, Arg24, Asp175, Asp287, Leu284, Ile328, His355, and the backbone atoms of residues Phe246 and Leu174 that form the putative oxyanion-hole. Sidechains were cut at the Cα-Cβ bond, except for the arginine, which was cut at the Cγ-Cδ position, and saturated with hydrogen atoms. The DFT models comprised *ca.* 140 atoms. The terminal parts of the protein residues were kept fixed during optimizations to simulate the constrains arising from the rigid protein framework. Geometry optimizations were performed at the B3LYP-D3/def2-SVP/ε=10 [17-21], and single point energy evaluations were performed at B3LYP-D3/def2-TYZVP with ε=10 and ε=4. Reaction pathways were optimized using a *chain-of-states* method[22,23]. All QM calculations were performed with TURBOMOLE version 7.1-7.3 [24].

Supplementary Table 1. *E. coli* strains with coexpressed proteins and major polyketide products.

Strain	Proteins	Major products
ES8	AntBDEFG	**SEK4**, **SEK4b**
ES10	AntB-I	**SEK4**, **SEK4b**
ES12	AntABDEFG	**mutactin**
ES13	AntABCDEFG	**mutactin**
ES14	AntABDEFGH	**SEK34b**
ES15	AntABDEFGHI	**SEK34b**
ES16	AntABCDEFGH	**SP^{EC}1**, **SP1**, **SP4**, **SP5**
ES17	AntABCDEFGHI	**AQ-256**, **SP1**, **SP^{EC}1**
ES65	AntABCDEFGH + Red1	***S*-DNPA**

Supplementary Table 2. Identification of polyketides using HPLC-UV-MS or NMR.

	$[M+H]^+$	$[M-H]^-$	RT^A / min	RT^B /min	identified with
SEK4	301[C]		5.3	6.5	authentic standard (Tsai lab) , UV
SEK4b	319		5.4	7.1	authentic standard (Tsai lab), UV
mutactin	303		6.3	10.2	authentic standard (Δ*antC* mutant), UV
SEK34	285[D]		6.0	9.5	UV
SEK34b	285		6.8		UV
DMAC (**SP^{EC}1**)		297	7.8		isolation and NMR, UV
SP1	302		6.2		UV, labeled media
SP4	240		8.2		labeled media
utahmycin A (**SP5**)	254		8.4		authentic standard (Brady lab)[25]
AQ-256		255	8.7		standard (TT01 wild type), UV
***S*-DNPA**	287		8.5		UV and MS; Ichinose lab[10]

A: HPLC gradient A; B: HPLC gradient B (described above); C: SEK4-H_2O; D: SEK34-H_2O

Supplementary Table 3. Crystallographic data collection and refinement statistics.

	AntI	AntI [SeMet (peak)]
Crystal parameters		
Space group	$C222_1$	$C222_1$
Cell constants	a= 54.1 Å	a= 54.1 Å
	b= 154.3 Å	b= 154.5 Å
	c= 91.2 Å	c= 91.2 Å
Subunits / AU[a]	1	1
Data collection		
Beam line	X06SA, SLS	X06SA, SLS
Wavelength (Å)	1.0	0.979
Resolution range (Å)[b]	30-1.85 (1.95 - 1.85)	30-1.9 (2.0 - 1.9)
No. observed reflections	221,122	220,792
No. unique reflections[c]	33,019*	57,339#
Completeness (%)[b]	99.7 (100)	98.4 (99.5)
R_{merge} (%)[b, d]	5.7 (56.0)	6.4 (51.6)
I/□ (I)[b]	18.9 (3.0)	11.7 (2.7)
Refinement (REFMAC5)		
Resolution range (Å)	30-1.85	
No. refl. working set	31,340	
No. refl. test set	1,649	
No. non hydrogen	3,253	
Solvent (H_2O, PEG, glycerol)	205	
R_{work} / R_{free} (%)[e]	16.8 / 20.4	
r.m.s.d. bond (Å) / (°)[f]	0.003 / 0.79	
Average B-factor (Å^2)	37.1	
Ramachandran Plot (%)[g]	98.1 / 1.9 / 0	
PDB accession code	6HXA	

[a] Asymmetric unit

[b] The values in parentheses for resolution range, completeness, R_{merge} and I/σ (I) correspond to the highest resolution shell

[c] Data reduction was carried out with XDS and from a single crystal. *Friedel pairs were treated as identical reflections; #Friedel pairs were treated as individual reflections

[d] $R_{merge}(I) = \Sigma_{hkl}\Sigma_j \mid I(hkl)_j - \langle I(hkl)\rangle \mid / \Sigma_{hkl}\ \Sigma_j\ I(hkl)_j$, where $I(hkl)_j$ is the j^{th} measurement of the intensity of reflection hkl and $\langle I(hkl)\rangle$ is the average intensity

[e] $R = \Sigma_{hkl} \mid |F_{obs}| - |F_{calc}| \mid / \Sigma_{hkl} |F_{obs}|$, where R_{free} is calculated without a sigma cut off for a randomly chosen 5% of reflections, which were not used for structure refinement, and R_{work} is calculated for the remaining reflections

[f] Deviations from ideal bond lengths/angles

[g] Number of residues in favored region / allowed region / outlier region

Supplementary Table 4. Primers used for the plasmid construction and genotype verification. Restriction sites are underlined.

plasmid	primer 5` to 3`	vector
ZQ6	TACTAACATATGGACGATATTTCTTTATCATCTGATT	pSU18
	GTCAATGTCGACTATTACTCATCTTTGTTCCTTATAATCTCG	
ZQ9	ACTTGCAGATAACGATTTTC	pJET1.2/blunt
	ACATTCCTGGCCATTTAT	
ZQ10	TAGTTCCATATGAAATATGCCTTTATTACCGG	pSU18
	CTTGAAGTCGACCCATTGGGTATATGAAATCTCTTT	
ZQ11	TAGTTCCATATGAAATATGCCTTTATTACCGG	pSU18
	TTCTCAGTCGACTTCCCAAAAATCACAATCTATAGG	
ZQ12	ACTTGCAGATAACGATTTTC	pJET1.2/blunt
	CTATTGGGTTTATTTTTATTATTCATCT	
ZQ13	ACTTGCAGATAACGATTTTC	pJET1.2/blunt
	TTACCATCGCGATGTATATT	
ZQ16	TACTAACATATGGACGATATTTCTTTATCATCTGATT	pSU18
	CTTGAAGTCGACCCATTGGGTATATGAAATCTCTTT	
ZQ40	AAAATAGAATTC**C**ATGAATAATAAAAATAAACCCAATAGA	pCOLA Duet-1
	GTATAACTGCAGTCAATTAACCTTTTTTATAGCCA	
ZQ40_S245A	[Phos]CTTTTGGTGGTTATTTTGC	pCOLA Duet-1
	CAATTCCTAAGAAACAAAGAAG	
ZQ40_D326A	[Phos]GAAAGTGAAAAAATTAGATCAAC	pCOLA Duet-1
	GCGATCTGAAATATATCATCTAA	
ZQ40_D327A	[Phos]CTATATTTCAGATCGATAAAGTG	pCOLA Duet-1
	CATCTAATTCACCATGAAC	
ZQ40_H355A	[Phos]CTGTTTGCTTAAATAAAATAAACG	pCOLA Duet-1
	CAGCCTCTGATTCATAACATAA	
ZQ62	TAATTAGAATTCCGTGATAATAAATAACAGAAATGAATCTCAACC	pACYC Duet-1
	TCCTTTCTGCAGGTTACTAAATACGAGTGTCTAACCACT	
ZQ76	TAGTTCGAATTC**C**ATGAAATATGCCTTTATTACCGG	pCDF Duet-1
	ATGACACTGCAGTTATTATAATATTGCGACCACTC	
ZQ80	No primers, more information in method section.	pCOLA Duet-1
pDS_plu4186	GGTCAAGCATGCGTGGGTGATAGCTATATTAATATCG	pDS132
	TTCACTGAGCTCCCCAATCTGAAACTTGTATCAT	
pDS_plu4188	AACTTAGCATGCCTCCGCAATCTATTGCTAAC	pDS132
	CGAGATGAGCTCCCAGTGGCAAACCACTC	
pDS_plu4192	[11]	pDS132
	primers for verification PCR	
vP_plu4186_Fw	GTGATTCAGTAAAAGTCATTTATAATG	
vP_plu4186_Rv	GCCAGTTAATACCTCAGCAG	
vP_plu4188_Fw	GCGCTTTAGTAATCAAGGTC	
vP_plu4188_Rv	GCTGAGAATTGATTTTAATTACG	
vP_plu4192_Fw	TACCTTATGGATTTCAAGATGC	
vP_plu4192_Rv	AACTCTTTGTTATTGCCATCAC	
pDS132fw	GATCGATCCTCTAGAGTCGACCT	
pDS132rv	ACATGTGGAATTGTGAGCGG	

Supplementary Table 5. Plasmids used in this work. *: gene *antI* with selected mutation. **: codon optimized for *E. coli* expression.

plasmid	genotype	reference
pJET1.2/blunt	pMB1ori, Ap^r	Fermentas
pSU18	P15A ori, Cm^r, *lacZ* promoter	[26]
pACYC Duet-1	P15A ori, Cm^r, T7*lac* promoter	Novagen
pCOLA Duet-1	ColA ori, Km^r, T7*lac* promoter	Novagen
pCDF Duet-1	CDF ori, Sm^r, T7*lac* promoter	Novagen
pDS132	*pir* dependent, Cm^r, *oriT*, *oriV*, *sacB*	[27]
ZQ6	P15A ori, Cm^r, *antB*, *lacZ* promoter	this work
ZQ9	pMB1 ori, (Ap^r), *antDEFG* with native promoter	this work
ZQ10	P15A ori, Cm^r, *antABC*, *lacZ* promoter	this work
ZQ11	P15A ori, Cm^r, *antAB*, *lacZ* promoter	this work
ZQ12	pMB1ori, (Ap^r), *antDEFGH* with native promoter	this work
ZQ13	pMB1ori, (Ap^r), *antDEFGHI* with native promoter	this work
ZQ16	P15A ori, Cm^r, *antBC*, *lacZ* promoter	this work
ZQ40	ColA ori, Km^r, T7*lac* promoter, *antI*	this work
ZQ40_S245A	ColA ori, Km^r, T7*lac* promoter, *antI**	this work
ZQ40_D326A	ColA ori, Km^r, T7*lac* promoter, *antI**	this work
ZQ40_D327A	ColA ori, Km^r, T7*lac* promoter, *antI**	this work
ZQ40_H355A	ColA ori, Km^r, T7*lac* promoter, *antI**	this work
ZQ62	P15A ori, Cm^r, T7*lac* promoter, *antDEFGH*	this work
ZQ76	CDF ori, SM^r, T7*lac* promoter, *antABC*	this work
ZQ80	ColA ori, Km^r, T7*lac* promoter, *actVI-ORF1***	this work
pDS_plu4186	*pir* dependent, Cm^r, *oriT*, *oriV*, *sacB,* partial *plu4186*	this work
pDS_4188	*pir* dependent, Cm^r, *oriT*, *oriV*, *sacB,* partial *plu4188*	this work
pDS_plu4192	*pir* dependent, Cm^r, *oriT*, *oriV*, *sacB,* partial *plu4192*	this work

Supplementary Table 6. *E. coli* strains (ES) used in this work.

strain	genotype	reference
E. coli DH10B		[28]
E. coli BL21 (DE3)		Novagen
E. coli s17-1 λpir		[29]
ES8	DH10B::ZQ9, ZQ6	this work
ES10	DH10B::ZQ13, ZQ16	this work
ES12	DH10B::ZQ9, ZQ11	this work
ES13	DH10B::ZQ9, ZQ10	this work
ES14	DH10B::ZQ12, ZQ11	this work
ES15	DH10B::ZQ13, ZQ11	this work
ES16	DH10B::ZQ12, ZQ10	this work
ES17	DH10B::ZQ13, ZQ10	this work
ES36	BL21 (DE3)::ZQ40	this work
ES53	BL21 (DE3)::ZQ62, ZQ76, ZQ40	this work
ES59	BL21 (DE3)::ZQ62, ZQ76, ZQ40_S245A	this work
ES61	BL21 (DE3)::ZQ62, ZQ76, ZQ40_D326A	this work
ES62	BL21 (DE3)::ZQ62, ZQ76, ZQ40_D327A	this work
ES64	BL21 (DE3)::ZQ62, ZQ76, ZQ40_H355A	this work
ES65	BL21 (DE3)::ZQ62, ZQ76, ZQ80	this work
ES27	s17-1 λpir::pDS_plu4186	this work
ES28	s17-1 λpir::pDS_4188	this work
ES29	s17-1 λ pir::pDS_4192	this work

Supplementary Table 7. *P. luminescens* TT01 wild type and mutants with genotypes and major products

TT01 strain	Genotype	Major products	Reference
WT	*P. luminescence* wild type	**AQ-256**, **AQ-270a**, **AQ-284a**	[30]
antI::cat	*antI* inactivated by plasmid insertion	**SP1**	this work
Δ*antC*	*antC* deletion	**SEK34**, **SEK34b**	this work
Δ*antH*	*antH* deletion	**mutactin**	[11]
antD::cat	*antD* inactivated by plasmid insertion	no polyketide	[11]

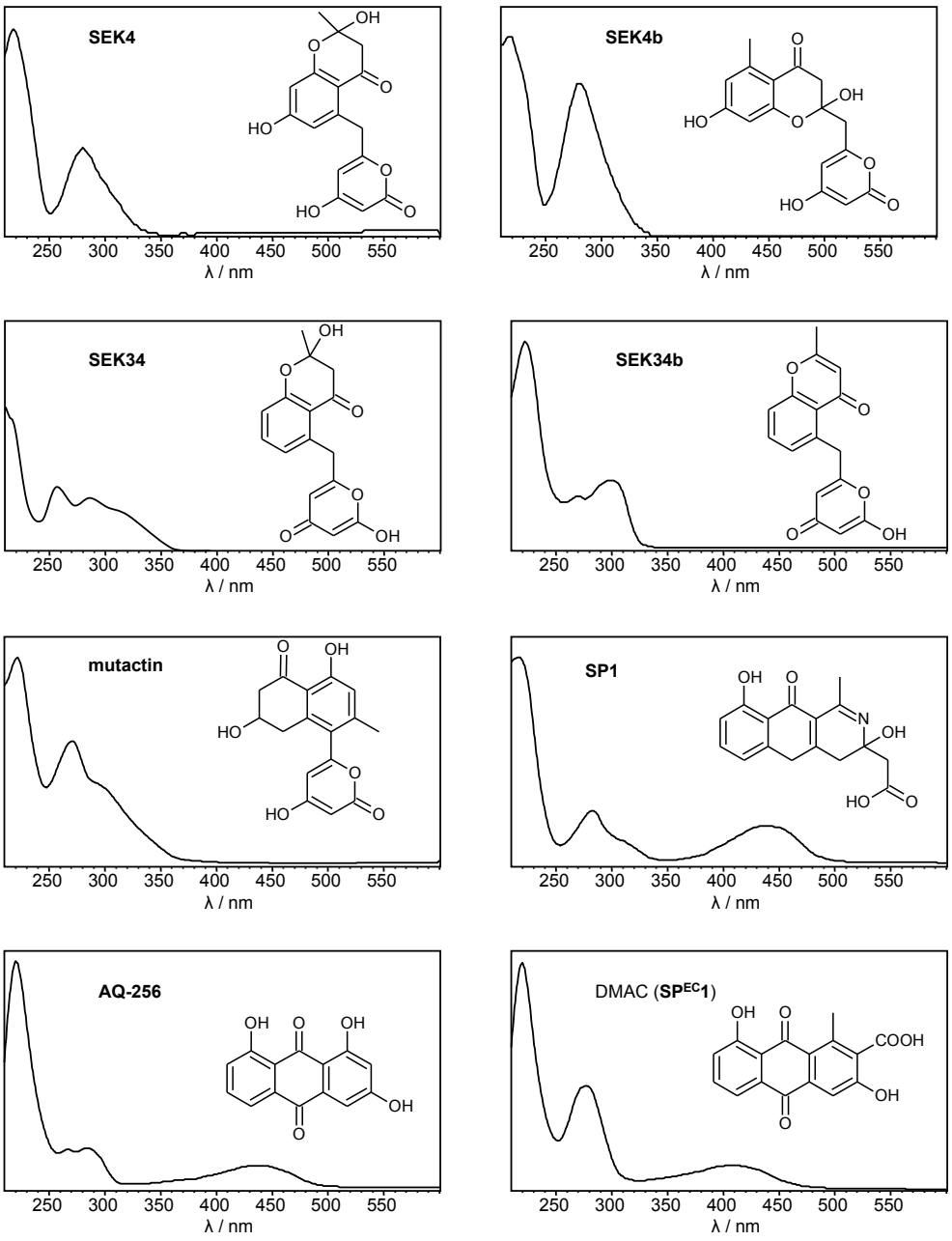

Supplementary Figure 1. UV spectra (λ: 210-600 nm) and structures of major shunt products produced by *E. coli* DH10B with *ant* genes.

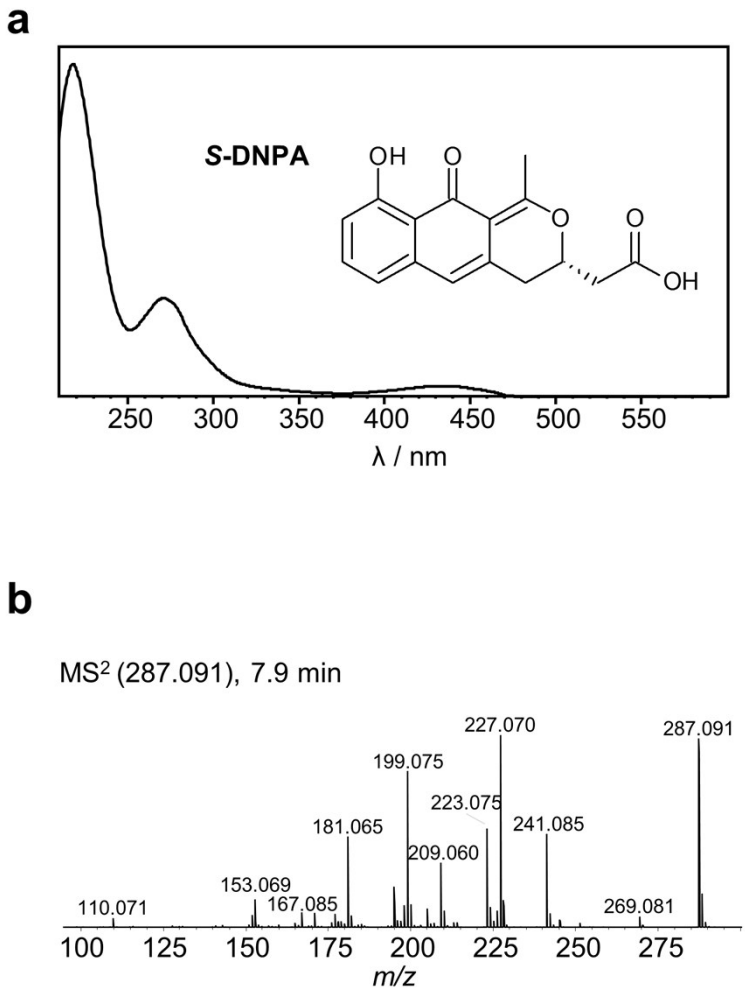

Supplementary Figure 2. a) UV (λ: 210-600 nm) and **b**) MS^2 spectra of *S*-DNPA produced by *E. coli* BL21 (DE3) with *antA-H* and the gene encoding for RED1. The sown data corresponds well with published data from the Ichinose lab.[10]

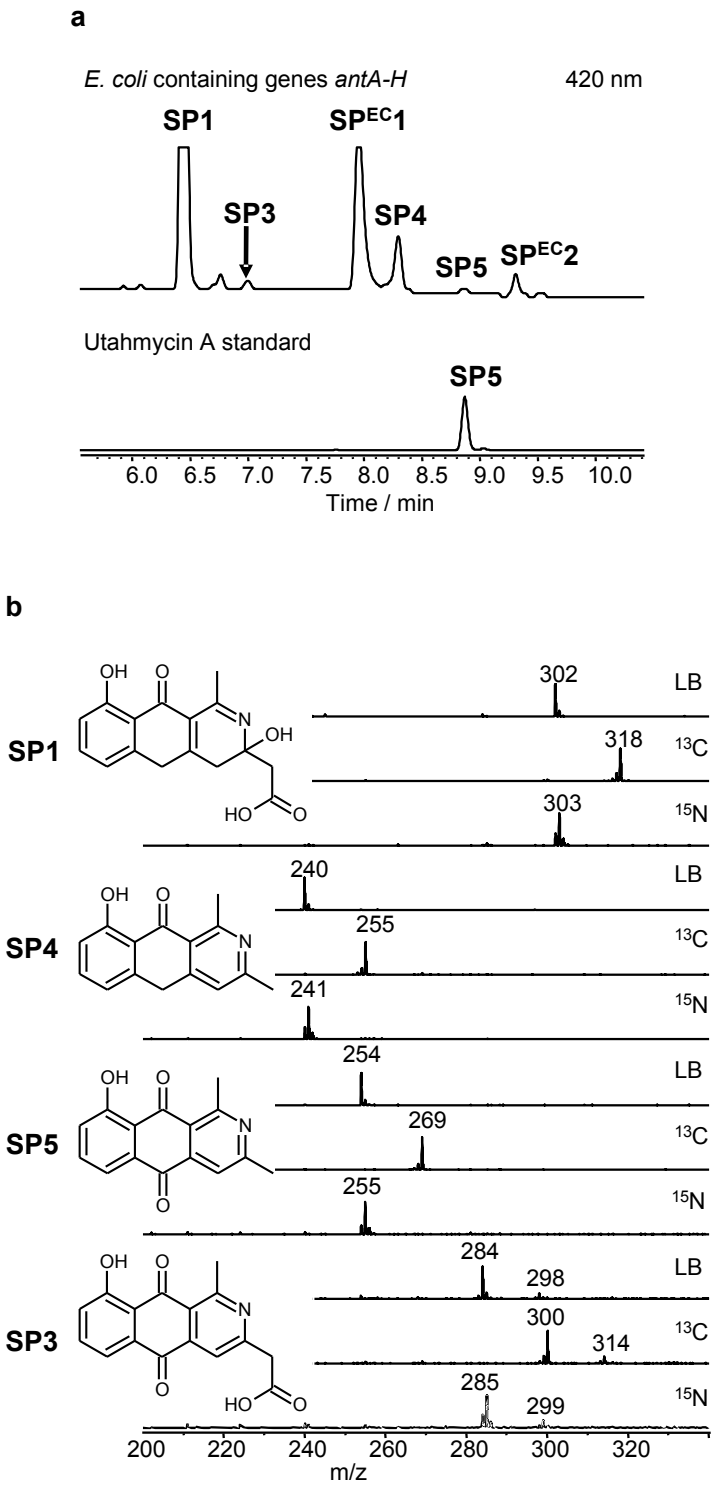

Supplementary Figure 3. (**a**) HPLC-UV analyses (420 nm) of extracts of heterologous expression of genes *antABCDEFGH* in *E. coli* DH10B (top) and authentic utahmycin A standard (bottom). (**b**) Determination of the number of carbon and nitrogen atoms for **SP1**, **SP4**, **SP5** and **SP3** using cultivation of the *E. coli* DH10B strain ES16 with genes *antABCDEFGH* in standard growth medium (LB medium, ^{14}N , ^{12}C, ^{16}O, ^{1}H), ^{15}N labeled medium (^{15}N , ^{12}C, ^{16}O, ^{1}H), or ^{13}C labeled medium (^{14}N , ^{13}C, ^{16}O, ^{1}H) as described previously. [31]

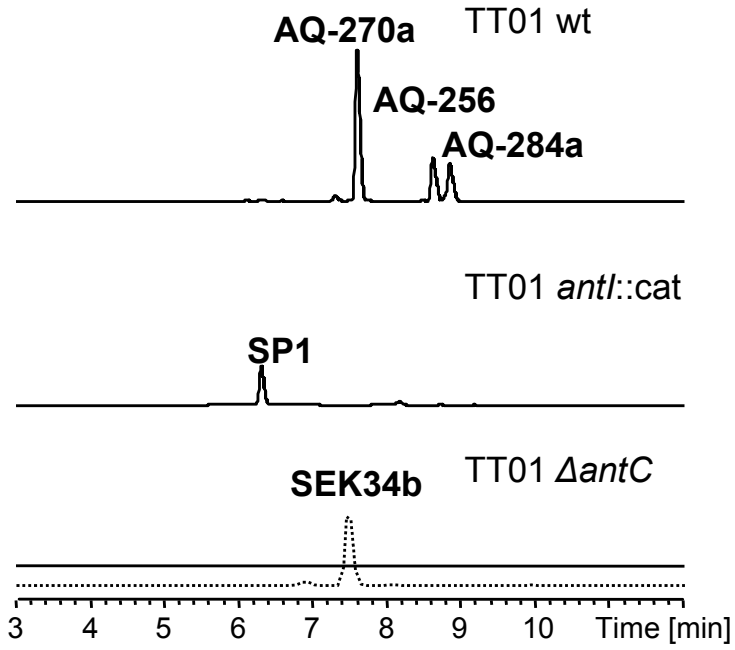

Supplementary Figure 4. HPLC-UV analyses (420 nm) of extracts of *P. luminescens* TT01 wild type, mutant *antI*::cat and mutant *ΔantC*. In both mutants, the wt AQs were not produced. A new shunt product **SP1** could be identified in the mutant *antI*::cat. In the mutant Δ*antC*, shunt product **SEK34b** could be identified with EIC (dotted line, m/z 285 $[M+H]^+$). See also Supplementary Table 7.

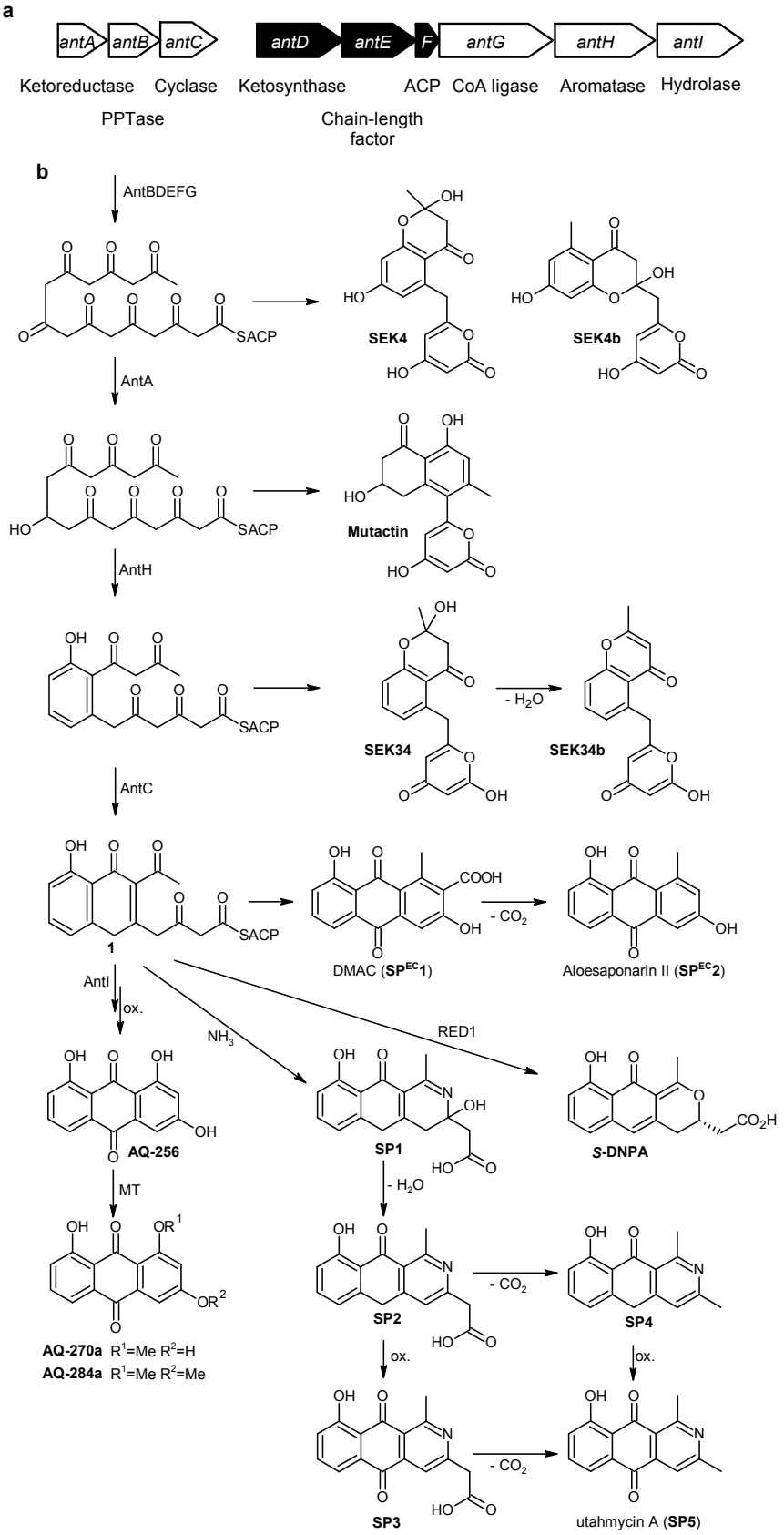

Supplementary Figure 5. Biosynthesis gene cluster *antABCDEFGHI* for the production of anthraquinones from *P. luminescens* (**a**) and proposed biosynthesis of all identified compounds (**b**) following classical type II PKS pathways. [32,33]

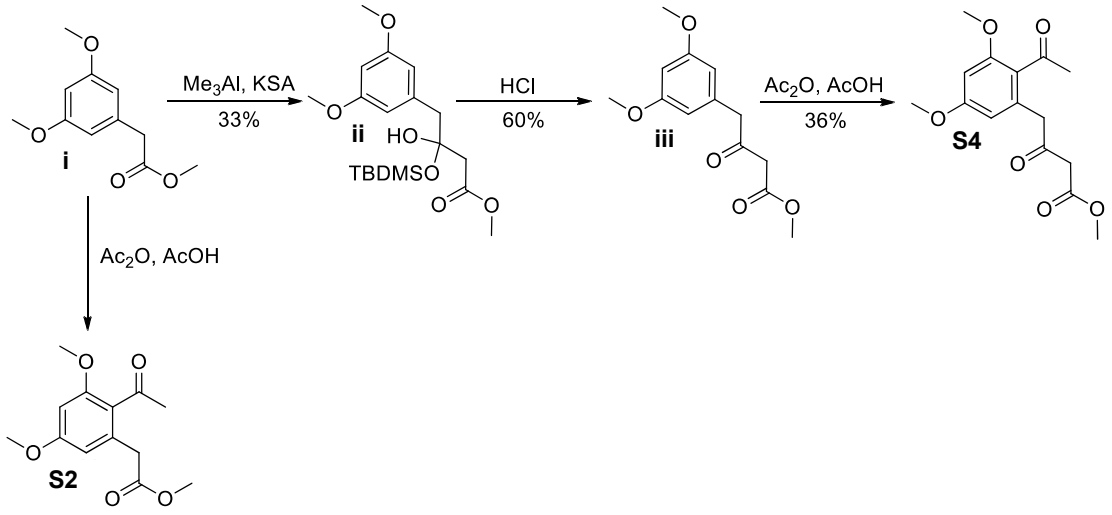

Supplementary Figure 6. Synthesis of model compounds **S2** and **S4**. KSA: tert-butyl((1-methoxyvinyl)oxy)dimethylsilane; Me_3Al: trimethylaluminium; AcOH: acetic acid; Ac_2O: acetic anhydride.

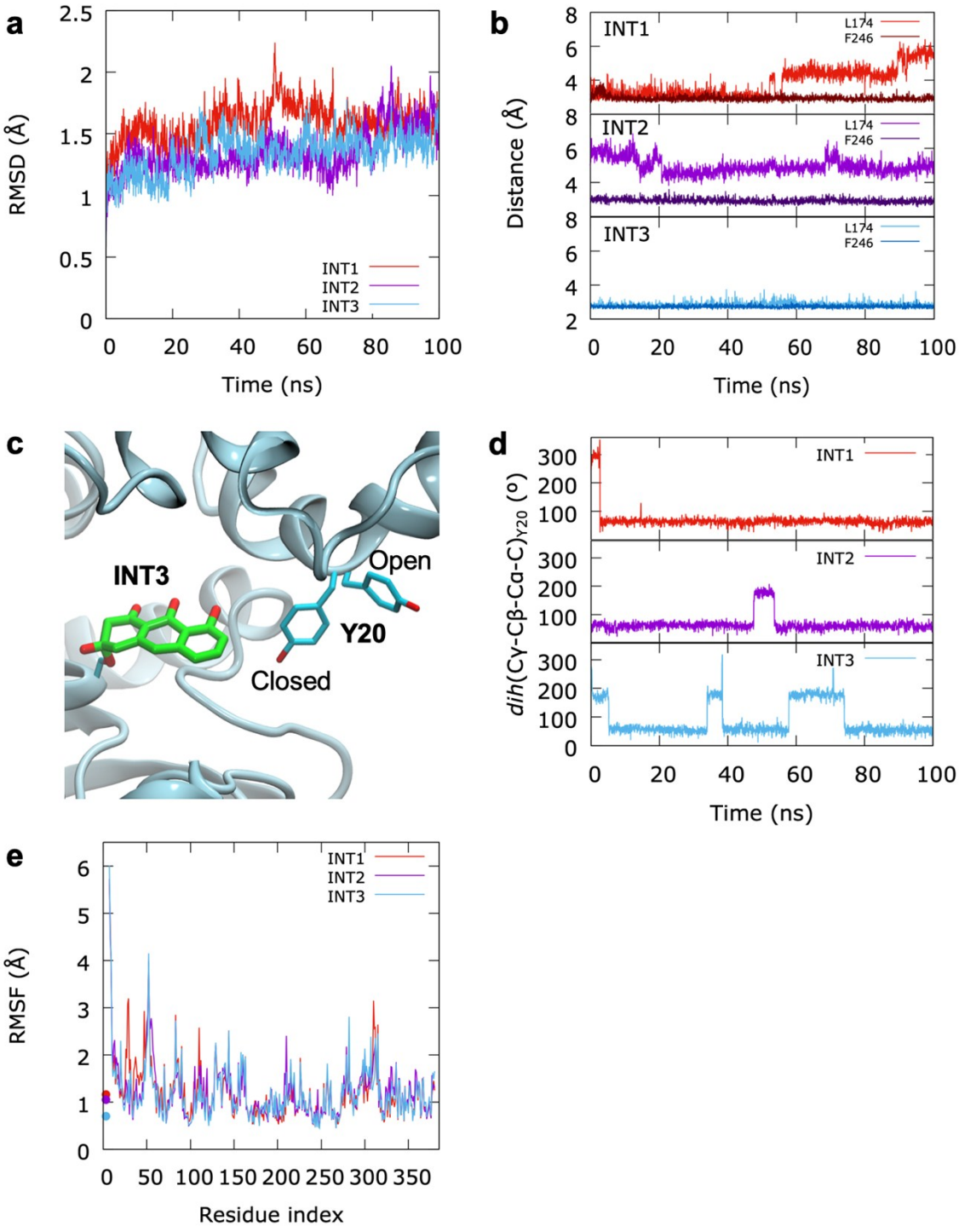

Supplementary Figure 7. Classical molecular dynamics simulations of intermediates **INT1**, **INT2**, and **INT3**, modeled in the active site of AntI. (**a**) RMSD for protein backbone atoms. (**b**) Distance between the oxyanion hole and backbone Leu174/Phe246. (**c**) Open and closed conformations of Tyr20 observed during the MD simulations. (**d**). Dynamics of the Tyr20 Cγ-Cβ-Cα-C dihedral angle during the MD simulations. A dihedral angle > 100º/< 100º corresponds to the open/closed conformations, respectively. (**e**) RMSF of protein residues (red/purple/blue lines), and the ligand, shown as a dot at residue index zero.

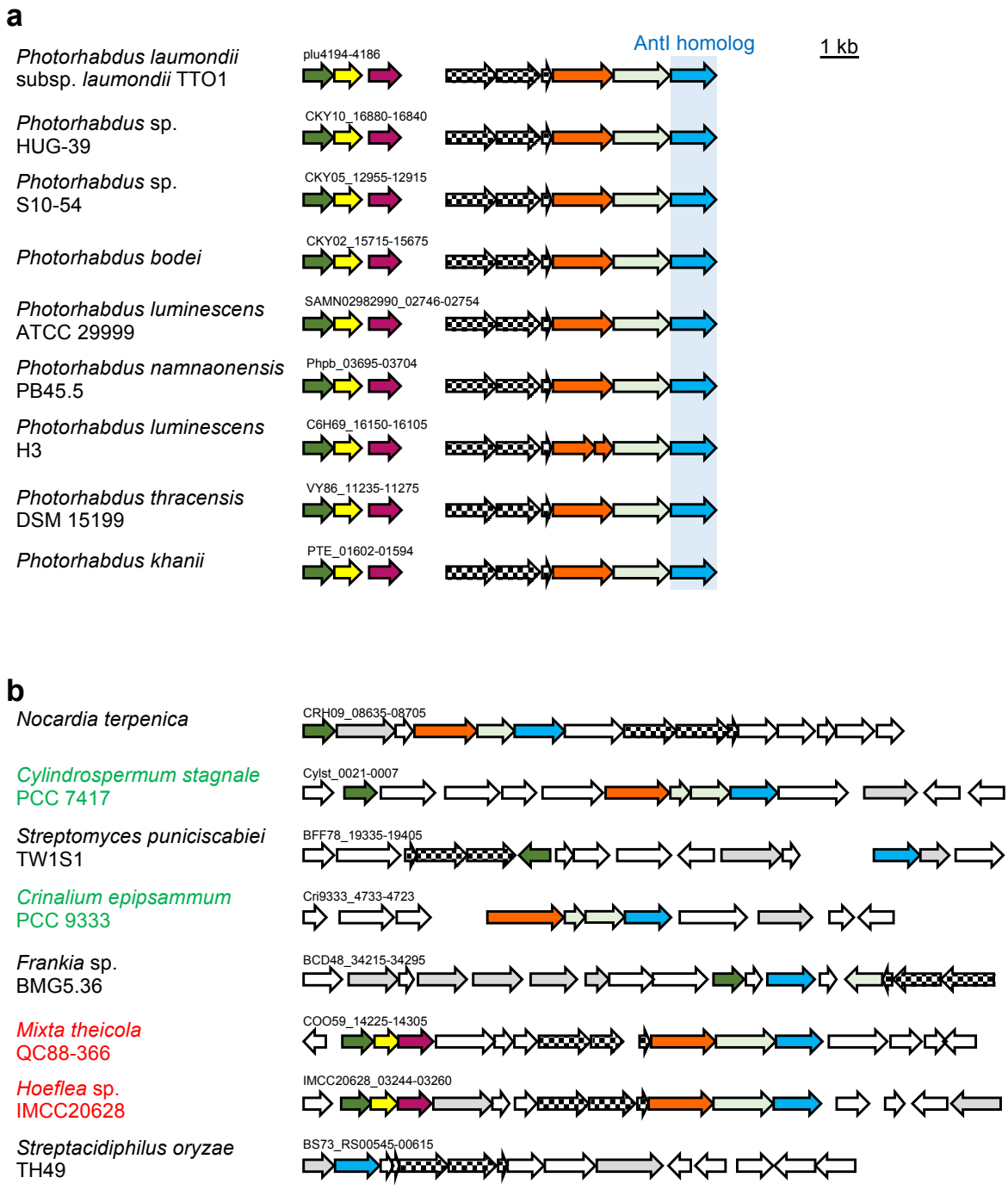

Supplementary Figure 8. Biosynthesis gene clusters related to *ant* from *P. luminescens* from other *Photorhabdus* strains (**a**) and other bacteria (**b**). Cyanobacteria are shown in green and other Gram-negative bacteria in red.

a

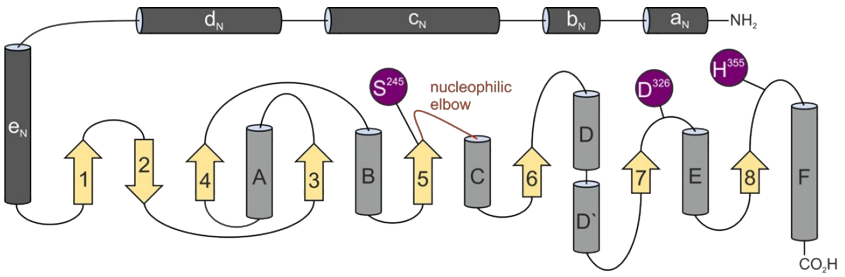

b

```
                                aN                                bN
AntI        MNNKNKPNRISPELLATCGYFMPRIFFLN--SQYAPQVHWGDVV---AALSH--FPAGNL   53
AYC1p       ------------------WILGDKFDTVFPHKGSLKVLWESRWKFACSKSVYPFHDGSI   41
WdYG1       --------------MATEKYYIRDAITKPAVHHESYQKLWETKWKKPCEMGVYPFMFGSI   46
                             : :   :      : : :  *       .  .   *  *.:

                                     cN                        dN
AntI        D-------------LSSEEFWYEWMINWSKVGDSYINIANSAKSEVS---HVRALRSAAA   97
AYC1p       EDFEPIFNHLISKNINDA-ASDEYTQAFLPTASALEEKAAQALQAGKHEEASNLLCRAAV  100
WdYG1       KDFEPVAQEIIKKGLKEPYDWDEYAQMYFPKAEELAKIAEEAEAAGEKEKASEYYLRSSA  106
            .            :..     *:   :   ..   : * .*    .     .    ::.
            dN                 eN                          1     2
AntI        CYHWAEFMYFSDRS-RKIQLR-------EYIRSCFLSSIKYSDLLVDHQYI-VVDKFHMP  148
AYC1p       VYRISRFPYVDITKPNSIKRVAFERQKQAYLKATSLWTQPIREVTVPHTYRTGNDGAHIP  160
WdYG1       VYRISRFPTPRSEK----QKYAWRKGCEVFYKGAALMEYPIKEVRIPHKHGIEGEGDVVP  162
             *: :.*      .    :          : :.  *      :: : * :    :   :*
            2          3              A          4
AntI        FFLIFPKGYKEEENHPLPCVILSNGLDSMTEIEILSLAEFFLGKNMAVAIFDGPGQGINL  208
AYC1p       IYIRTPAGA--DQSNPVPIVLIMTGLDGYRPDNSQR-THEILARGWAAVVAEIPGTADCP  217
WdYG1       VNFLLPPNA--SETSPVPCVLIITGLDGYRTELAVW-QQGWRSKGVATVIAEIPGTGDSP  219
            . :  * .   .:. *:* *:: .***.          .   .:. *..: : ** .
                       B          5          C          6
AntI        GKSPIAIDMELYVSSIVKLLEDDARINSNLLCFLGISFGGYFALRVAQRIGDKFCCIVNL  268
AYC1p       ADPADPASPDRLWDSVLSYLDQRPELNTAKMVVWGLSAGGYYAIRAAHTHRDRLLGAIAH  277
WdYG1       ALRQDPTSPDRQWSSVLDWIESQKAVDSKKIVAWGFSTGGYYALRMAHTHKDRLLATISL  279
            .      . :   .*::. ::.   :::  :   *:* ***:*:* *:   *::   :
                          D                    D`
AntI        SGGPEIAE-FDKLPRRLKEDFQFAFM------QDNSHM-------QSIFDEIKLDISLPC  314
AYC1p       GPGCHYYLDPEWLAKVNDHEYPFEITAAWATKHGYKTVEEFVAGAQKKFSLVETGIVDQP  337
WdYG1       GGGAHHMFDREWLEHANKLEYPFDLSNTLAYKFGYPDLESFIEE-SSKFSLLNDGTLQKP  338
            . * .     : * :  . :: * :        .   :       .. *. :: .
            7          E          8                F
AntI        KTKVFTVHGELDDIFQIDKVKKLDQLWGDNHQLLCYESEAHVCLNKINEYMIQVSDWVSE  374
AYC1p       SCRLLLLNGVDDGVVPIEDCLVLFEH-GSPKEGRFYKGLPHMGY---PNSLPV-------  386
WdYG1       CTKVLLVNGNDDEIFPIDDMFVSLEN-GQPKLARMVKGKKHMGE---PESFSIILEWIHK  394
              ::: ::*  * :. *:.     :  *. :     :.  *:      : :

            F
AntI        QFWLNGYKKG-----------  384
AYC1p       ----------------------  386
WdYG1       LLGLDGKIKEQLAMIPSRTKY  415
```

Supplementary Figure 9. AntI adopts α/β hydrolase fold (N-terminal domain in dark grey; C-terminal domain in grey). Helices and β-strands are represented as cylinders and arrows respectively. The nucleophilic elbow and the catalytic residues are highlighted. (**a**) Folding topology of AntI. (**b**) Multiple protein sequence alignment of AntI with Ayg1p from *Aspergillus fumigatus*[34] and WdYG1 from *Exophiala dermatitidis*[35] using Clustal Omega.

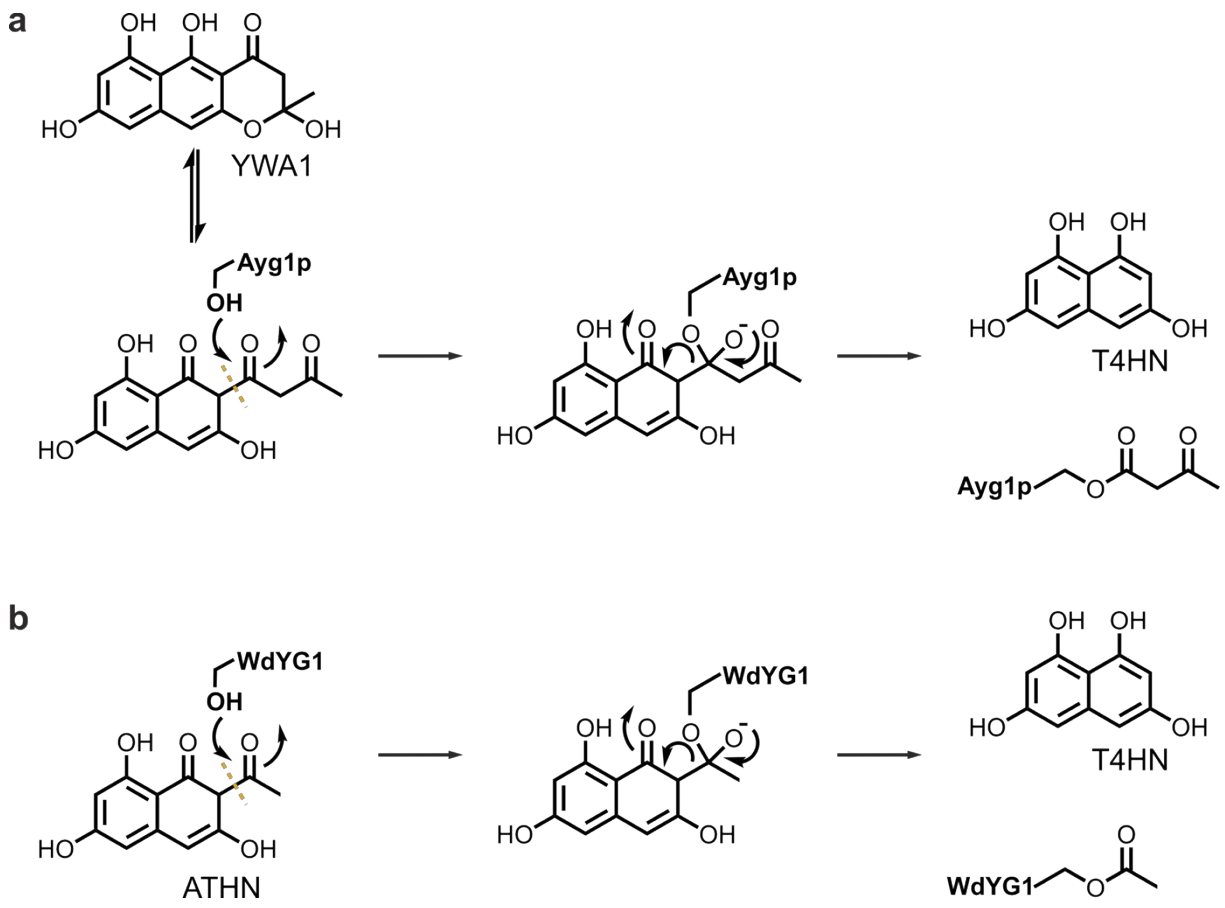

Supplementary Figure 10. Proposed polyketide shortening mechanism catalysed by Ayg1p (**a**) and WdYG1 (**b**) from *Aspergillus fumigatus* and *Exophiala dermatitidis*, respectively.

NMR spectra

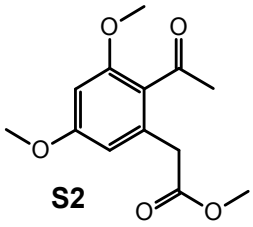

S2

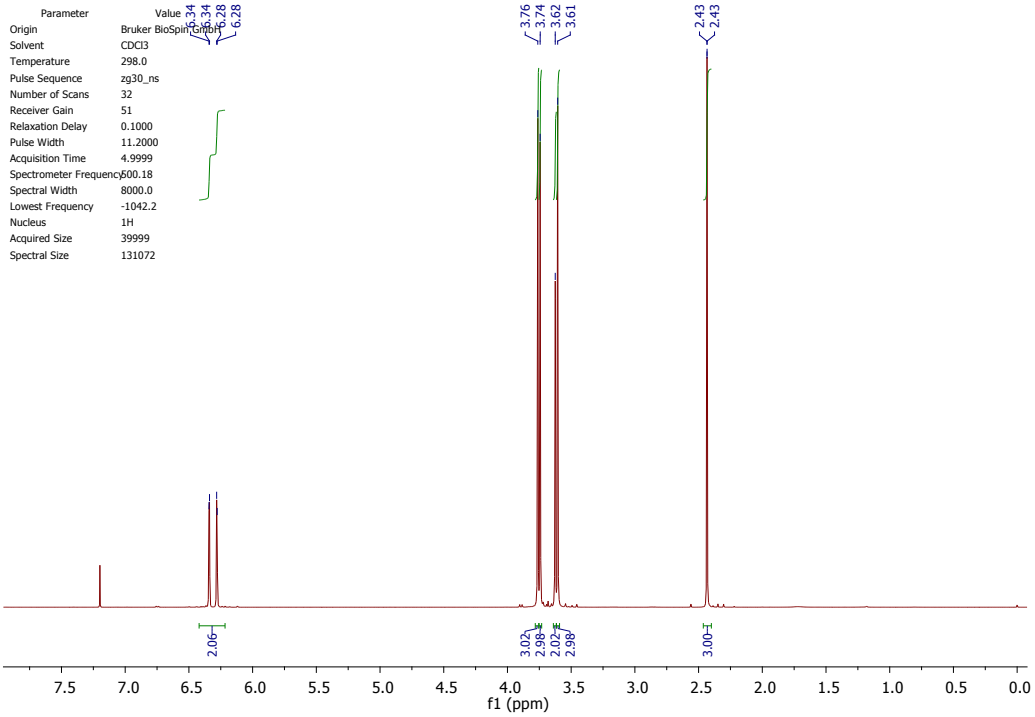

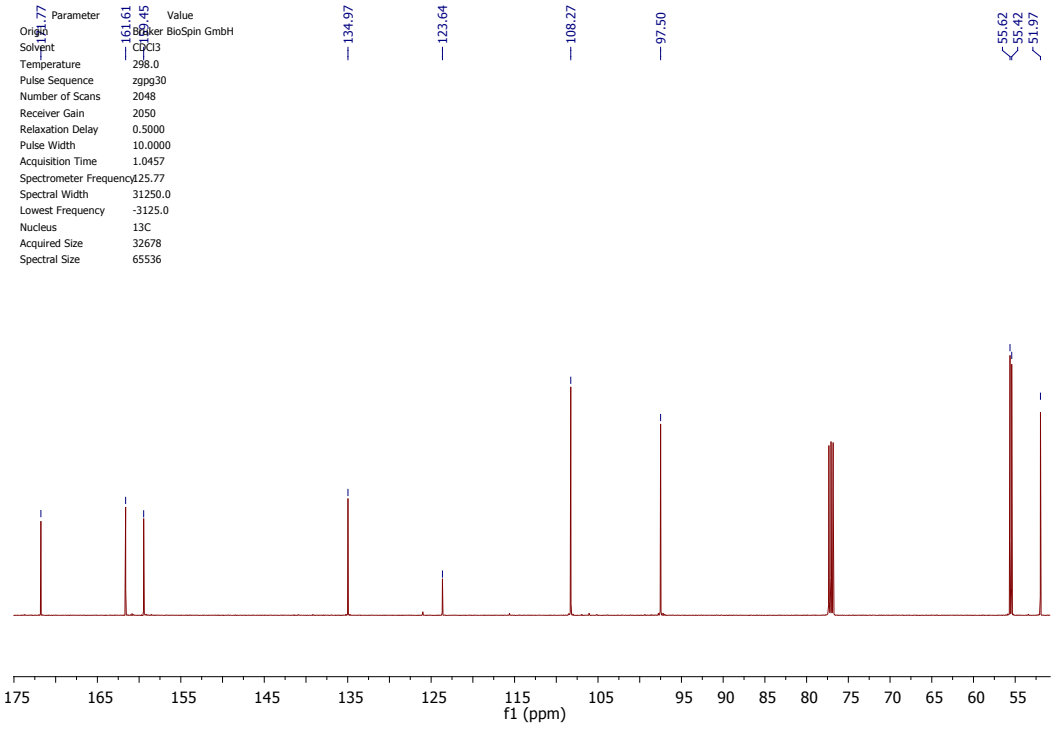

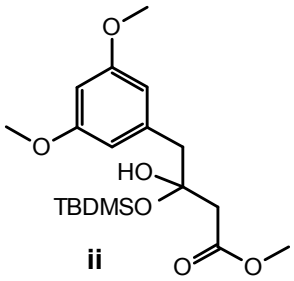
O
O
HO
TBDMSO
O
O

ii

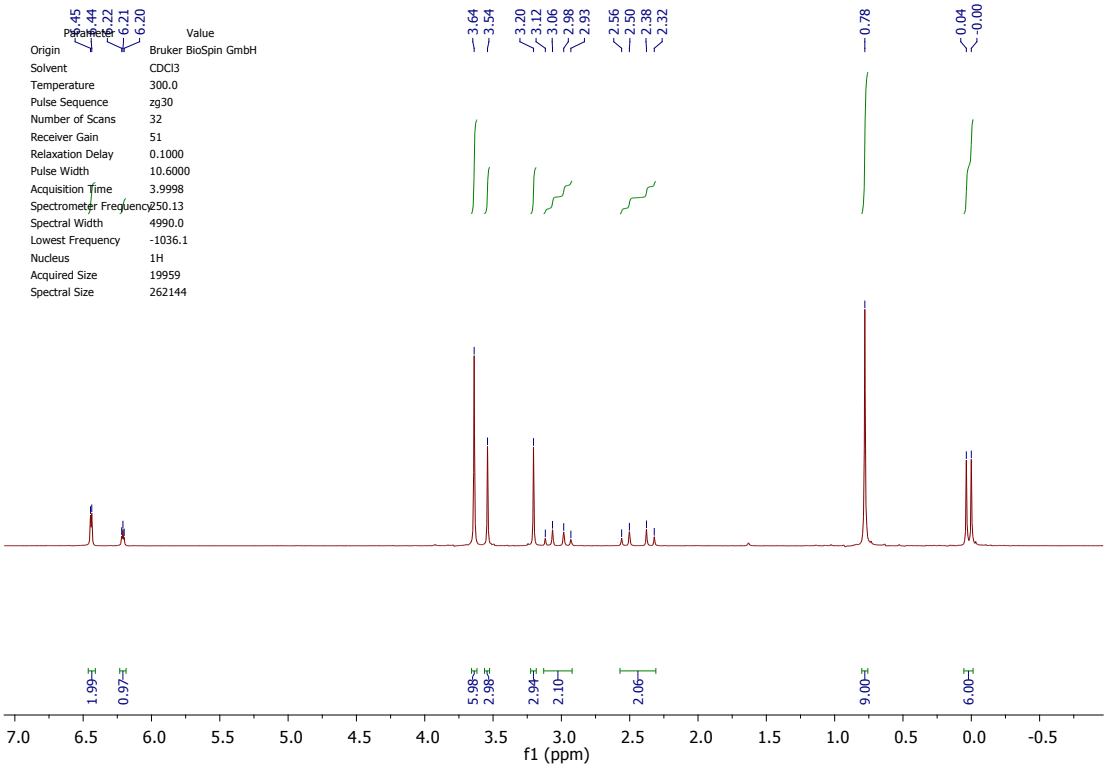
Parameter Value
Origin Bruker BioSpin GmbH
Solvent CDCl3
Temperature 300.0
Pulse Sequence zg30
Number of Scans 32
Receiver Gain 51
Relaxation Delay 0.1000
Pulse Width 10.6000
Acquisition Time 3.9998
Spectrometer Frequency 250.13
Spectral Width 4990.0
Lowest Frequency -1036.1
Nucleus 1H
Acquired Size 19959
Spectral Size 262144
6.45 6.44 6.22 6.21 6.20
3.64 3.54 3.20 3.12 3.06 2.98 2.93 2.56 2.50 2.38 2.32
0.78
0.04 -0.00
1.99 0.97 5.98 2.98 2.94 2.10 2.06 9.00 6.00
7.0 6.5 6.0 5.5 5.0 4.5 4.0 3.5 3.0 2.5 2.0 1.5 1.0 0.5 0.0 -0.5
f1 (ppm)

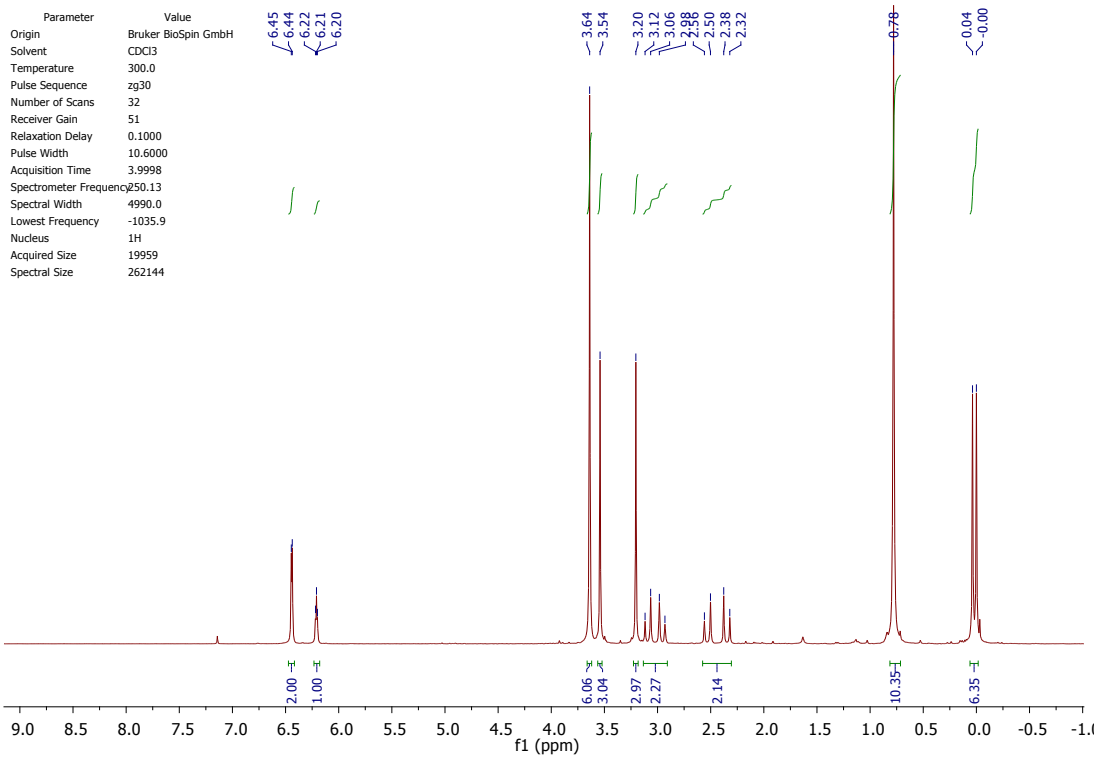
Parameter Value
Origin Bruker BioSpin GmbH
Solvent CDCl3
Temperature 300.0
Pulse Sequence zg30
Number of Scans 32
Receiver Gain 51
Relaxation Delay 0.1000
Pulse Width 10.6000
Acquisition Time 3.9998
Spectrometer Frequency 250.13
Spectral Width 4990.0
Lowest Frequency -1035.9
Nucleus 1H
Acquired Size 19959
Spectral Size 262144
6.45 6.44 6.22 6.21 6.20
3.64 3.54 3.20 3.12 3.06 2.98 2.93 2.50 2.38 2.32
0.78
0.04 -0.00
2.00 1.00 6.06 3.04 2.97 2.27 2.14 10.35 6.35
9.0 8.5 8.0 7.5 7.0 6.5 6.0 5.5 5.0 4.5 4.0 3.5 3.0 2.5 2.0 1.5 1.0 0.5 0.0 -0.5
f1 (ppm)

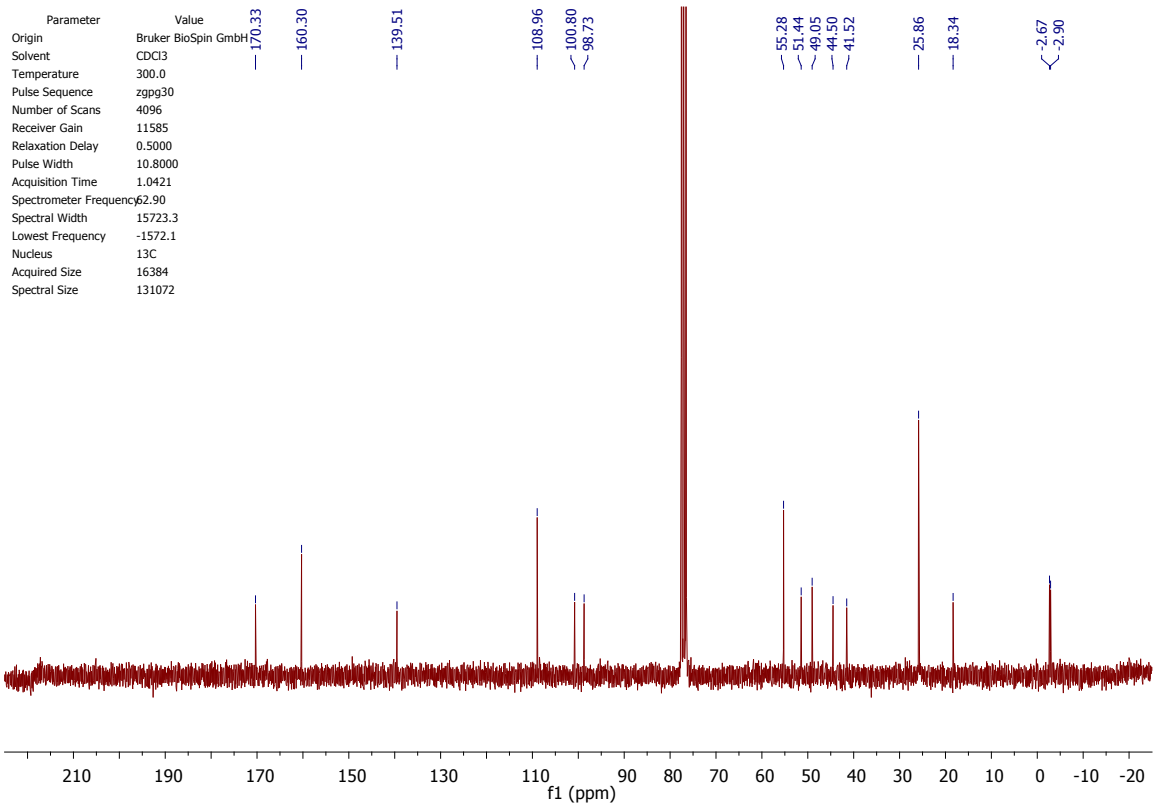
Parameter Value
Origin Bruker BioSpin GmbH
Solvent CDCl3
Temperature 300.0
Pulse Sequence zgpg30
Number of Scans 4096
Receiver Gain 11585
Relaxation Delay 0.5000
Pulse Width 10.8000
Acquisition Time 1.0421
Spectrometer Frequency 62.90
Spectral Width 15723.3
Lowest Frequency -1572.1
Nucleus 13C
Acquired Size 16384
Spectral Size 131072
170.33
160.30
139.51
108.96
100.80
98.73
55.28
51.44
49.05
44.50
41.52
25.86
18.34
-2.67
-2.90
210 190 170 150 130 110 90 80 70 60 50 40 30 20 10 0 -10 -20
f1 (ppm)

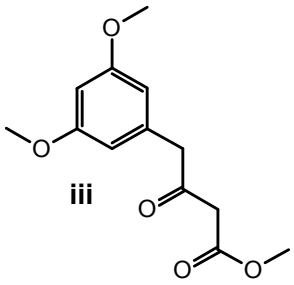

iii

Parameter	Value
Origin	Bruker BioSpin GmbH
Solvent	CDCl3
Temperature	298.0
Pulse Sequence	zg30_ns
Number of Scans	32
Receiver Gain	51
Relaxation Delay	0.1000
Pulse Width	11.2000
Acquisition Time	4.9999
Spectrometer Frequency	500.18
Spectral Width	8000.0
Lowest Frequency	259.0
Nucleus	1H
Acquired Size	39999
Spectral Size	131072

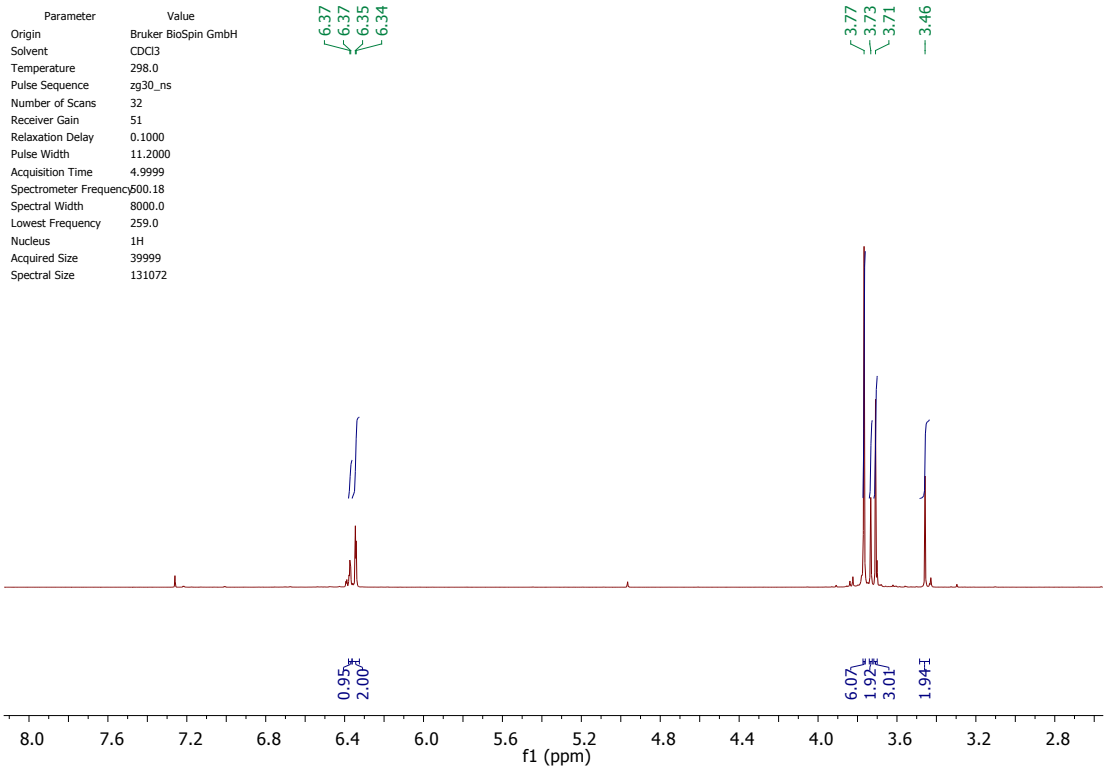

Parameter	Value
Origin	Bruker BioSpin GmbH
Solvent	CDCl3
Temperature	298.0
Pulse Sequence	zgpg30
Number of Scans	2048
Receiver Gain	2050
Relaxation Delay	0.5000
Pulse Width	10.0000
Acquisition Time	1.0457
Spectrometer Frequency	125.77
Spectral Width	31250.0
Lowest Frequency	-3125.0
Nucleus	13C
Acquired Size	32678
Spectral Size	65536

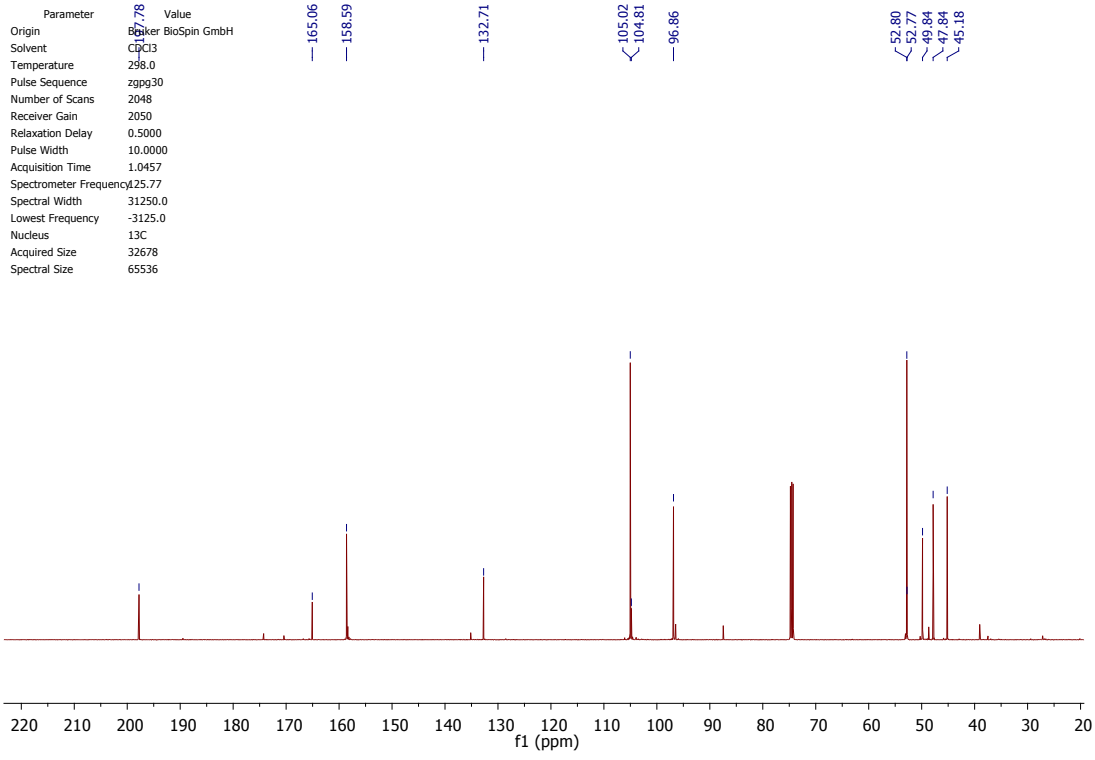

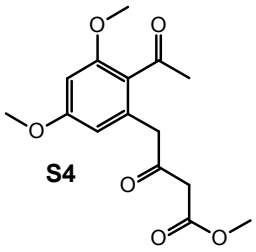

Parameter	Value
Origin	Bruker BioSpin GmbH
Solvent	CDCl3
Temperature	298.2
Pulse Sequence	zg30_ns
Number of Scans	32
Receiver Gain	45
Relaxation Delay	0.1000
Pulse Width	11.2000
Acquisition Time	3.9999
Spectrometer Frequency	500.18
Spectral Width	10000.0
Lowest Frequency	-2044.7
Nucleus	1H
Acquired Size	39999
Spectral Size	131072

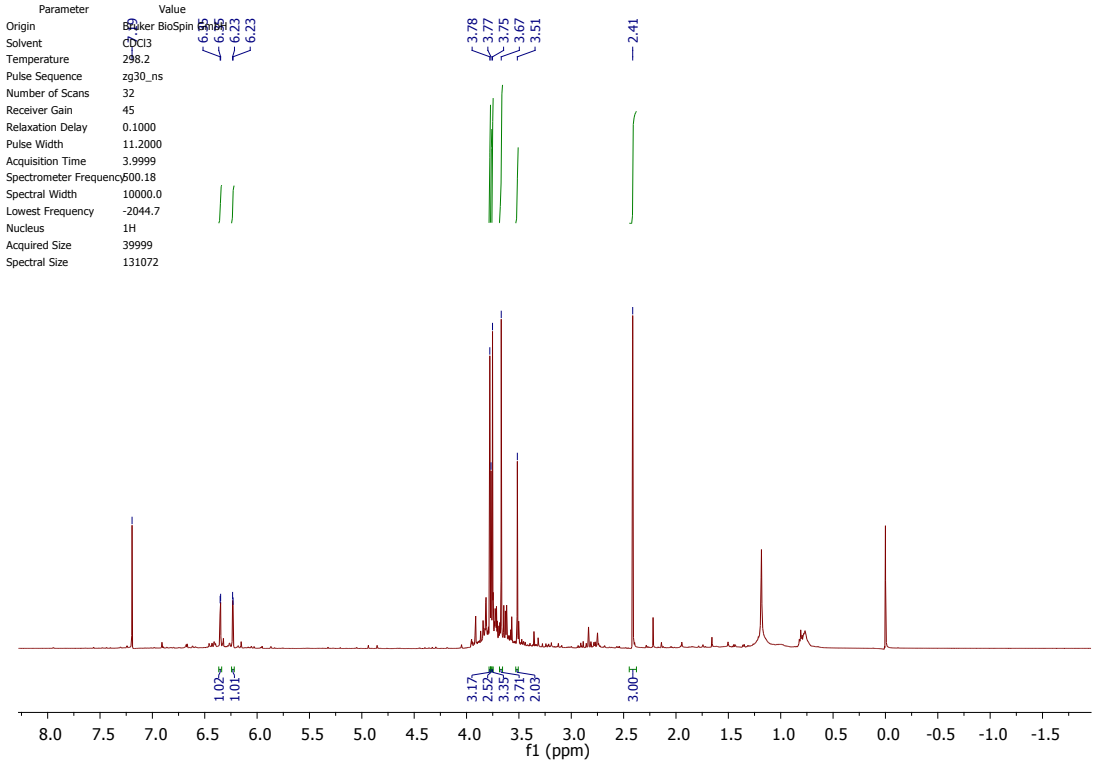

Parameter	Value
Origin	Bruker BioSpin GmbH
Solvent	CDCl3
Temperature	298.0
Pulse Sequence	deptqsp
Number of Scans	1024
Receiver Gain	2050
Relaxation Delay	2.0000
Pulse Width	10.0000
Acquisition Time	1.0486
Spectrometer Frequency	125.77
Spectral Width	31250.0
Lowest Frequency	-3125.0
Nucleus	13C
Acquired Size	32768
Spectral Size	65536

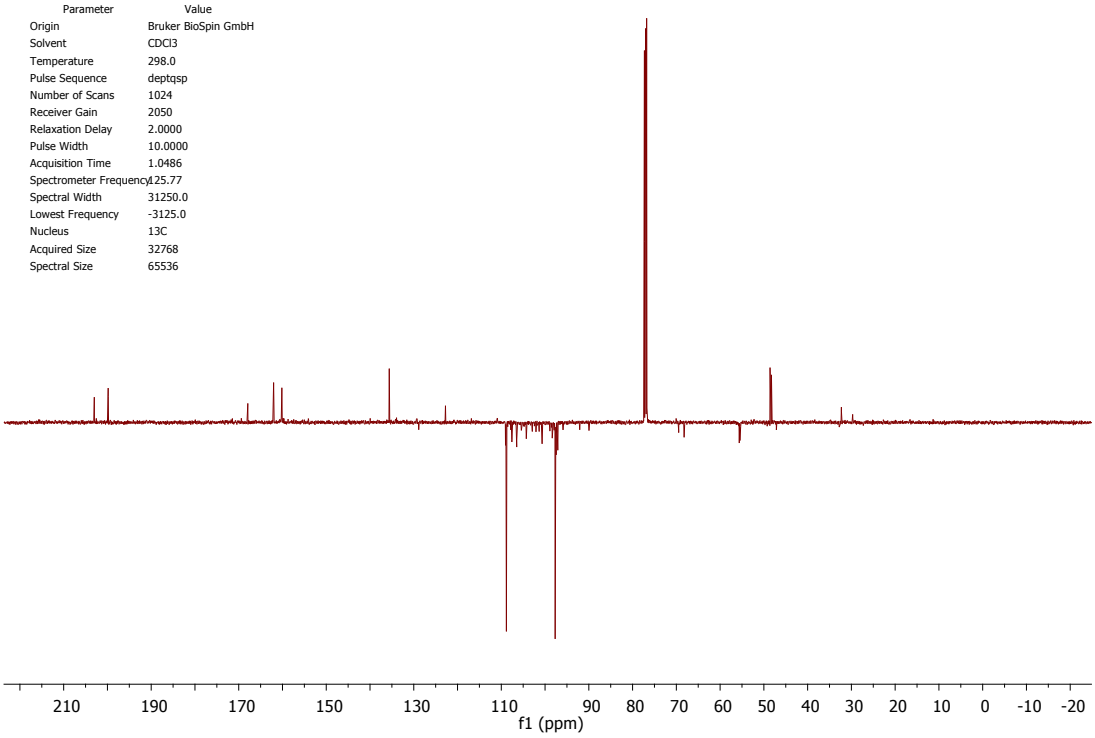

References

1. Gaitatzis, N., Hans, A., Müller, R. & Beyer, S. The mtaA Gene of the Myxothiazol Biosynthetic Gene Cluster from Stigmatella aurantiaca DW4/3-1 Encodes a Phosphopantetheinyl Transferase that Activates Polyketide Synthases and Polypeptide Synthetases. **129,** 119–124 (2001).
2. Van Duyne, G. D., Standaert, R. F., Karplus, P. A., Schreiber, S. L. & Clardy, J. Atomic structures of the human immunophilin FKBP-12 complexes with FK506 and rapamycin. *J Mol Biol* **229,** 105–124 (1993).
3. Kabsch, W. XDS. *Acta Crystallogr D Biol Crystallogr* **66,** 125–132 (2010).
4. Sheldrick, G. M. A short history of SHELX. *Acta Crystallogr., A, Found. Crystallogr.* **64,** 112–122 (2008).
5. McCoy, A. J. *et al.* Phaser crystallographic software. *J Appl Crystallogr* **40,** 658–674 (2007).
6. Cowtan, K. *Joint CCP4 ESF-EACBM Newsletter on Protein Crystallography (Daresbury Laboratory, Warrington, UK)*. **31,** 34–38 (1994).
7. Murshudov, G. N. *et al.* REFMAC5 for the refinement of macromolecular crystal structures. *Acta Crystallogr D Biol Crystallogr* **67,** 355–367 (2011).
8. Turk, D. MAIN software for density averaging, model building, structure refinement and validation. *Acta Crystallogr D Biol Crystallogr* **69,** 1342–1357 (2013).
9. Emsley, P., Lohkamp, B., Scott, W. G. & Cowtan, K. Features and development of Coot. *Acta Crystallogr D Biol Crystallogr* **66,** 486–501 (2010).
10. Itoh, T. *et al.* Actinorhodin biosynthesis: structural requirements for post-PKS tailoring intermediates revealed by functional analysis of ActVI-ORF1 reductase. *Biochemistry* **46,** 8181–8188 (2007).
11. Brachmann, A. O. *et al.* A Type II Polyketide Synthase is Responsible for Anthraquinone Biosynthesis in *Photorhabdus luminescens*. *ChemBioChem* **8,** 1721–1728 (2007).
12. Larkin, M. A. *et al.* Clustal W and Clustal X version 2.0. *Bioinformatics* **23,** 2947–2948 (2007).
13. Huang, J. & MacKerell, A. D., Jr. CHARMM36 all-atom additive protein force field: Validation based on comparison to NMR data. *J. Comput. Chem.* **34,** 2135–2145 (2013).
14. Vanommeslaeghe, K. *et al.* CHARMM general force field: A force field for drug-like molecules compatible with the CHARMM all-atom additive biological force fields. *J. Comput. Chem.* **91,** NA–NA (2009).
15. Phillips, J. C. *et al.* Scalable molecular dynamics with NAMD. *J. Comput. Chem.* **26,** 1781–1802 (2005).
16. Humphrey, W., Dalke, A. & Schulten, K. VMD: visual molecular dynamics. *J Mol Graph* **14,** 33–8– 27–8 (1996).
17. Becke, A. D. Density‐functional thermochemistry. III. The role of exact exchange. *The Journal of Chemical Physics* **98,** 5648–5652 (1993).
18. Lee, C., Yang, W. & Parr, R. Development of the Colle-Salvetti correlation-energy formula into a functional of the electron density. *Phys. Rev., B Condens. Matter* **37,** 785–789 (1988).
19. Schäfer, A., Horn, H. & Ahlrichs, R. Fully optimized contracted Gaussian basis sets for atoms Li to Kr. *The Journal of Chemical Physics* **97,** 2571–2577 (1992).
20. Grimme, S., Antony, J., Ehrlich, S. & Krieg, H. A consistent and accurate ab initioparametrization of density functional dispersion correction (DFT-D) for the 94 elements H-Pu. *The Journal of Chemical Physics* **132,** 154104–20 (2010).

21. Klamt, A. & Schüürmann, G. COSMO: a new approach to dielectric screening in solvents with explicit expressions for the screening energy and its gradient. *J. Chem. Soc., Perkin Trans. 2* 799–805 (1993). doi:10.1039/P29930000799
22. Plessow, P. Reaction Path Optimization without NEB Springs or Interpolation Algorithms. *J. Chem. Theory Comput.* **9,** 1305–1310 (2013).
23. E, W., Ren, W. & Vanden-Eijnden, E. String method for the study of rare events. *Phys. Rev., B Condens. Matter* **66,** 251–4 (2002).
24. Ahlrichs, R., Bär, M., Häser, M., Horn, H. & Kölmel, C. Electronic structure calculations on workstation computers: The program system turbomole. *Chemical Physics Letters* **162,** 165–169 (1989).
25. Bauer, J. D., King, R. W. & Brady, S. F. Utahmycins a and B, azaquinones produced by an environmental DNA clone. *J. Nat. Prod.* **73,** 976–979 (2010).
26. Bartolomé, B., Jubete, Y., Martínez, E. & la Cruz, de, F. Construction and properties of a family of pACYC184-derived cloning vectors compatible with pBR322 and its derivatives. *Gene* **102,** 75–78 (1991).
27. Philippe, N., Alcaraz, J.-P., Coursange, E., Geiselmann, J. & Schneider, D. Improvement of pCVD442, a suicide plasmid for gene allele exchange in bacteria. *Plasmid* **51,** 246–255 (2004).
28. Grant, S. G., Jessee, J., Bloom, F. R. & Hanahan, D. Differential plasmid rescue from transgenic mouse DNAs into Escherichia coli methylation-restriction mutants. *Proc. Natl. Acad. Sci. U.S.A.* **87,** 4645–4649 (1990).
29. Simon, L. D., Randolph, B., Irwin, N. & Binkowski, G. Stabilization of proteins by a bacteriophage T4 gene cloned in Escherichia coli. *Proc. Natl. Acad. Sci. U.S.A.* **80,** 2059–2062 (1983).
30. Duchaud, E. *et al.* The genome sequence of the entomopathogenic bacterium Photorhabdus luminescens. *Nat Biotechnol* **21,** 1307–1313 (2003).
31. Bode, H. B. *et al.* Determination of the absolute configuration of peptide natural products by using stable isotope labeling and mass spectrometry. *Chem. Eur. J.* **18,** 2342–2348 (2012).
32. Hertweck, C. The Biosynthetic Logic of Polyketide Diversity. *Angew. Chem. Int. Ed.* **48,** 4688–4716 (2009).
33. Hertweck, C., Luzhetskyy, A., Rebets, Y. & Bechthold, A. Type II polyketide synthases: gaining a deeper insight into enzymatic teamwork. *Nat Prod Rep* **24,** 162 (2007).
34. Fujii, I. *et al.* Hydrolytic polyketide shortening by ayg1p, a novel enzyme involved in fungal melanin biosynthesis. *Journal of Biological Chemistry* **279,** 44613–44620 (2004).
35. Wheeler, M. H. *et al.* New Biosynthetic Step in the Melanin Pathway of Wangiella (Exophiala) dermatitidis: Evidence for 2-Acetyl-1,3,6,8-Tetrahydroxynaphthalene as a Novel Precursor. *Eukaryotic Cell* **7,** 1699–1711 (2008).